

Pilot Study: The analysis of known physical mixtures mimicking heroin samples using X-Ray Powder Diffraction for the purpose of qualitative and quantitative analysis.

Thulashija Sriskantharajah

08004268

MPhil Thesis- March 2023

Supervisors: Dr Andy Platt & Professor Andrew Jackson



Table of Contents

1. Introduction	5
1.1 Drugs of abuse and control	5
1.2 Forensic Investigation Techniques- Heroin	8
1.3 Presumptive tests	1
1.4 Gas Chromatography	2
1.5 High Performance Liquid Chromatography	3
1.6 X-Ray Powder Diffraction	4
2. X-Ray Spectroscopy.....	5
2.1 Analysis modes.....	7
2.2 Quantitative data analysis - Rietveld refinement	7
2.3 Beam damage.....	14
2.4 Sample preparation	14
2.5 Transmission analysis method development	16
2.6 Quantification using Rietveld refinement	19
3. Results and Discussion	20
3.1 Beam damage.....	21
3.2 Sample preparation	24
3.3 Transmission analysis method development	26
3.4 Quantification using Rietveld refinement	30
4. Bibliography	37

Figure 1 Roadmap for seized drug analysis as reported in OSAC seized drugs subcommittee (34)	0
Figure 2 Schematic diagram displaying Bragg's law.	6
Figure 3- Pure phase of Paracetamol using Reflection and Transmission setup	20
Figure 4 illustrates the differences in diffraction data for Paracetamol analysed using Reflection and Transmission mode.....	21
Figure 5 Comparison of damage between run 5 vs run 1 for Paracetamol	24
Figure 6 Comparison of ground Corundum (red trace), non-ground Corundum (blue trace) and difference between ground and non-ground Corundum (gold trace).	25
Figure 7 Comparison of a 50:50 caffeine:paracetamol physical mixture analysed using a 0.2mm slit size (red trace)and a 0.6mm slit size (blue trace). The green trace highlights the difference between the 0.2mm and 0.6mm slit diffractograms.	27
Figure 8 Transmission method optimisation for physical mixture ; Grey line = T2A5I5, Blue line = T1A5I5, Orange line= T1A1I1.	28
Figure 9 Transmission method optimisation for physical mixture zoomed between 10-40°; Grey line = T2A5I5, Blue line = T1A5I5, Orange line= T1A1I1.	28
Figure 10 Effect of changing analysis increment size and runtime on the accuracy and presicion of the Rietveld refinement	30

Table 1 Seizures of Opioids in 2018 as reported in the European Drug Report 2020: Trends and Developments (5)	5
Table 2 Bruker XRD instrument setting-	13
Table 3 sample preparation used in this study	15
Table 4 Analysis method used for transmission method optimisation	17
Table 5 Methods used for Reflection mode	19
Table 6 Comparison of the %-difference obtained for the main peaks of paracetamol, caffeine and codeine in repeated analysis.	23
Table 7 data show quantification of samples with and without internal standard.	32
Table 8 shows the quantification results obtained	33

Abstract

The illegal use of drugs is a major issue, and it is estimated that globally 210 million people aged 15-64 had used an illicit substance at least once. Heroin is one of the most problematic drugs and there is a high fatality rate as a result. The increasing trend in global seizures suggests that there is an increase in production of heroin. Current drug analysis involves qualitative and quantitative determinations using techniques such as Gas Chromatography (GC) and/ or Liquid Chromatography- Mass Spectrometry (LC-MS). Profiling of suspected drugs requires a further evaluation of the chromatographic and spectroscopic data along with further testing. The use of XRPD for the purpose of drug analysis is rare in the field of Forensic Science. It is a non-destructive technique preserving the sample analysed for further investigation if required. This study aims to demonstrate the capability of X-Ray Powder Diffractometry as a tool for simultaneous qualitative and quantitative analysis of known physical mixtures mimicking heroin samples.

A suitable method was developed to analyse known mixtures containing caffeine, codeine and paracetamol using the Bruker D8 Advance X-ray diffractometer. Following this the method was optimised to improve the qualitative and quantitative capabilities. The data highlighted that a 20 minute runtime using a 0.020° increment size provided accurate and repeatable data using a 50:50 caffeine:paracetamol mixture. Rietveld refinement was used to enable quantitation and provided highly accurate and repeatable results through single (active) component quantitation in the presence of an internal standard over a range of 12.6% w/w to 50.1% w/w.

1. Introduction

1.1 Drugs of abuse and control

The illicit use of narcotic drugs has become a major problem around the globe and has been on the rise. The world’s drug report 2020 highlighted a significant increase in the use of illicit drugs across both the proportion of the world’s population and overall numbers that uses illicit drugs. It is estimated that 210 million people (4.8% of the global population) used drugs at least once in 2019 (1,2).

According to the World Drug Report 2022, the total global opium production has shown an upward trend between 2017 and 2021 with an increase between 7-8 tons. Whilst this is produced in over 50 countries, three countries contributed to approximately 97% of the global production for the past five years. Afghanistan contributed approximately 87% of the global production and supplied to markets in Europe, Middle-East, South Asia and Africa. Total of 992 tons of opium was seized between 2016 and 2020, which is considerably lower than other illicit substances such as cocaine, cannabis and new psychoactive substance (1,3,4).

The quantity of opiate seizures in Europe has shown to be 9.7 tonnes in 2018 which is an increase from 5.7 tons from 2016 (5). Table 1 shows the most common opioids seized include heroin, methadone, buprenorphine, tramadol and other medicinal opioids (1,6,7). In comparison, cannabis and cocaine seizures correlates to 79% of the total drug seizures reported across Europe in 2018. Whilst the seizure of heroin and other opioids reported to be 5%, it remains to be one of the more harmful forms of use i.e. injecting (1).

Table 1 Seizures of Opioids in 2018 as reported in the European Drug Report 2020: Trends and Developments (5)

		Quantity				Number of countries
		Kilograms	Litres	Tablets	Patches	
Heroin	37000	9700			29	
Methadone	1 650	130.9	26.4	34 500	20	

Buprenorphine	3 220	0.2		106 500		18
Tramadol	5 520	0.7		1 112 300		14
Fentanyl derivatives	930	6.2	0.1	19 800	587	13
Morphine	1 110	354.1	0.2	12 400		12
Opium	550	781.2				15
Codeine	510	0.3		28 400		12

In the UK opioids and particularly heroin remain associated with the greatest health and social harms. Although there is a decline in the use of heroin, it is the most commonly reported primary substance of use among those seeking treatment (8,9).

1.1.1 Legislation

In general, the Misuse of Drugs Act 1971 is the primary legislation in the United Kingdom for the drug control and the controlled substances have been grouped into three classes (A, B and C), which provides a basis for attributing penalties for offences. Drugs of abuse were grouped into three classes in the 1971 Act, but in 1985 the "Misuse of Drugs Act Regulations" classified drugs of abuse into five Schedules (10). The first Schedule includes natural drug products, such as cannabis, the majority of which are hallucinogens. Drugs which can be manufactured by synthesis or semi-synthesis from natural starting materials in illegal laboratories, have been classified into Schedule 2. These are collectively known as stimulants and narcotic analgesics, such as amphetamine and heroin (diamorphine), respectively. The drugs in Schedules 3, 4 and 5, which include, for example, prescription drugs are considered less dangerous than the drugs in Schedules 1 and 2. Unlawful possession of Class A drugs such as heroin, cocaine involves penalties of up to 6 months imprisonment and/or a fine however, possession with intend to supply could reach up to 7 years (11-13).

The Drug Trafficking Act 1994 outlines drug trafficking including transporting and storing, importing or exporting, manufacturing or supplying drugs enclosed by the Misuse of Drugs

Act 1971 (6). For trafficking in Class A drugs, the maximum penalty of 'life' imprisonment. the number of drug law offences such as use/possession and supply was estimated to be 106,862 in 2015/2016 (13). If a control could be maintained over the countries such as Afghanistan, this would improve one of the world's most intractable drug problem (14). However previous experiences had shown that it is difficult to achieve this goal.

1..1.2 Heroin

Heroin is a mixture that contains diamorphine; it is arguably the most problematic drug (15). It is used by 13 million to 21 million of those aged 15-64 worldwide. The amount of heroin estimated to be imported annually into the UK is between 18-23 tonnes. The vast majority of this is derived from Afghan opium. Pakistan is a major transit country for Afghan opiates with well-established ethnic and familial links to the UK (16). Heroin trafficked via Pakistan to the UK is likely to have either been sent directly by parcel, air courier or maritime container; or been trafficked by sea onto eastern or southern Africa for onward movement. Iran is another important gateway for Afghan opiates, which are trafficked west from Afghanistan, often en route to Turkey and western Europe (1,2,17) Opiates also leave Afghanistan and enter Central Asia; however, this routing primarily supplies the Russian heroin market, and little is thought to be directed at the UK from this 'northern route'. In Europe, the Balkans is an important transport nexus with crime groups utilising long-established trafficking routes, while the Netherlands plays a strategically important role for organising the importation of heroin into the UK market (1,4).

Heroin is produced from the *Papaver somniferum* L. plant and can cause acute and chronic health problems. Moreover, heroin is mostly administered by injection, resulting in the spread of blood-borne diseases such as HIV/AIDS (16). It is estimated that, since 1980, 90% of the World's heroin supply comes from Afghanistan. In the last decade, about 380,000 kg of heroin was produced in a few provinces in Afghanistan, which was exported all around the world. There is a threat of a constant increase in the heroin market, leading to an increase in health problems and an increase in fatality as a result of it (18,19). Raw opium is a complex mixture containing sugars, proteins, fatty acids, water and approximately 40 alkaloids. The most common fatty acids are palmitic, linoleic, oleic, and stearic acids. The most common

alkaloids found in opium include (i) morphine (ii) codeine, (iii) thebaine, (iv) noscapine, (v) papaverine (11).

The synthesis of heroin dates back to the end of the 19th Century i.e. diamorphine was prepared for the first time in 1847. Typically, diamorphine is prepared by acetylation of morphine but a direct acetylation of opium compound has also been reported.(20,21,22) Unlike other class A drugs, an illicit heroin is a complex mixture and contains both acetylated and unacetylated opium alkaloids and after the process of purification, adulterants are added (20,23,24). Several acetylated impurities such as acetyl morphine and acetyl codeine are formed during the synthesis of heroin. The term 'heroin purity' always refers to the diamorphine content and is used commonly as a major component and it is deemed to be most effective pharmacologically. Morphine and codeine are effective 'pain killers' (20,25,26).

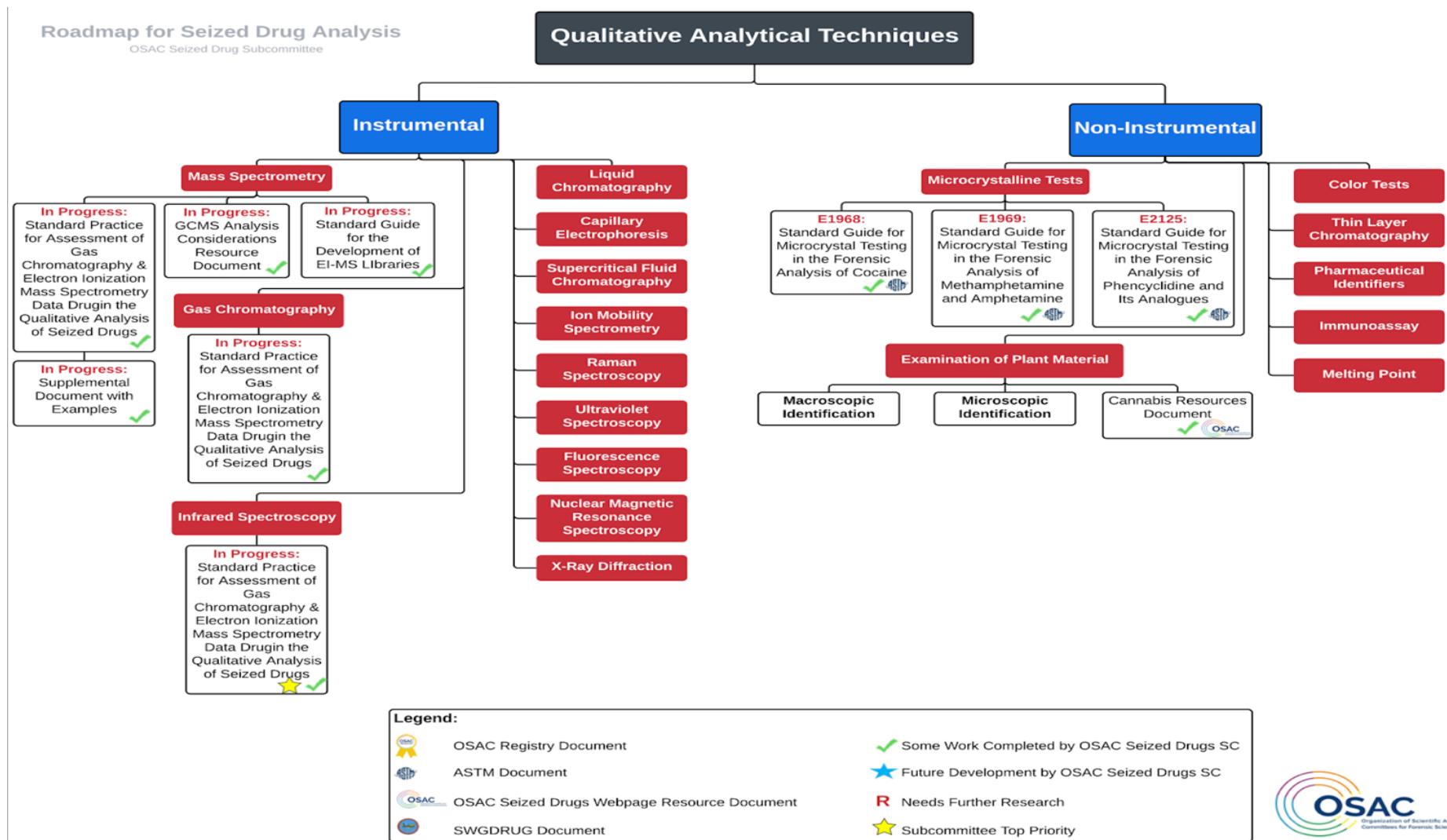
Two differently sourced heroin samples do not have the exact chemical characteristics. Profiling of illicit heroin is not performed infrequently but several studies have been performed, e.g. in the Netherlands and in Germany over the past 20 years. Heroin comparisons are made on the basis of the main compounds, the synthetic impurities and adulterants (27).

The most common adulterants of heroin samples are caffeine, baking soda, boric acid, cornstarch, dextrose, mannitol, paracetamol and sugars (lactose and glucose). Opiates and heroin depress the activity of the nervous system, including such reflexes as coughing, breathing and heart rate. Heroin, like other narcotics, gives a feeling of warmth by causing widening of the blood vessels (28-30). It also relieves stress and discomfort by creating a relaxed detachment from pain, desires and activity. Physical dependence and tolerance develop rapidly. (31,32)

1.2 Forensic Investigation Techniques- Heroin

For the purpose of investigation, case progression and possible prosecution the need for a rapid analysis of seized drugs is high. The main requirement in a forensic analysis consists of identification of the unknown substance and the need to quantify (purity percentage of the drug content) the substance if it is controlled. This needs to be performed whilst maintaining

the appropriate preservation and documentation requirements for judicial bodies. Additional requests can include the determination of chemical features common to other seizures for the purpose of intelligence gathering, e.g. profiling (26,33). The OSAC subcommittee has provided a roadmap to deliver a standard for the different types of drug analysis requested and conducted, see Figure 1 (34).



Legend:

OSAC Registry Document	✓ Some Work Completed by OSAC Seized Drugs SC
ASTM Document	★ Future Development by OSAC Seized Drugs SC
OSAC Seized Drugs Webpage Resource Document	R Needs Further Research
SWGDRUG Document	★ Subcommittee Top Priority

Organization of Scientific Area
Committees for Forensic Science

Figure 1 Roadmap for seized drug analysis as reported in OSAC seized drugs subcommittee (34)

The identification of active compounds of a sample, quantitative analysis and comparative analysis has been given a much more significant role in the area of drug analysis in Forensic Science. The chemical signature and chemical impurity profiling are used as a complimentary for the purpose of evidential and for intelligence purposes. According to the Drugs Characterisation/Impurity Profiling by UNODC indicates that in addition to the presence of pharmacophore, samples may contain one or more of these key components: (25,35)

1. Natural components- reminiscence of raw materials present in plant-based drugs (e.g. cocoa leaf, opium)
2. Synthetic impurities
3. Intermediates
4. By-products
5. Cutting agents

Examination of all of the components of a sample could provide a characteristic chemical signature can be assigned to every drug sample and thus play a key role in characterising samples. This information generated from the characterisation of drugs can be used to provide more general intelligence information such as identification of local/ regional / international source and distribution routes. It can confirm a link between two or more samples in drug supply offences and to aid prosecution purposes. According to the drug sampling guidelines by ENFSI the forensic investigation of illicit drugs is based on the determination of chemical and physical characteristics are divided into identification, quantification, chemical characterisation and chemical impurity profiling (12,29,33).

1..2.1 Presumptive tests

Initial analysis should be a physical description of the suspected sample. The physical observation should include information such as (i) colour, (ii) shape, (iii) weight, (iv) package and (v) marking/label. Seizures that contain crystalline substances should be examined to determine whether the suspected sample is homogenous or composed of different components. Determination of the physical characteristics such as the colour can be subjective.

Following a physical examination, the first 'presumptive test' for the identification of a drug acts as a fast screening procedure and those are typically colour tests (36). The use of these tests are an effective first in the identification of the drug classes. These techniques are based on the development of colour following reaction of the drug with chemical reagents. There are a number of general reagents available, although few are specific to a class of drugs. The three presumptive tests carried out for Opium based alkaloids are Marquis, Mecke and Frohde. Even though, presumptive tests are used as an indicative analysis because of (i) ease of use, (ii) cost effectiveness and (iii) less time consuming; there are number of disadvantages such as non-specificity of the colour reaction and relative insensitivity therefore further confirmatory tests are often required.

Thin Layer Chromatography (TLC) has been used in drug analysis to identify members of a drug class. The method used depends on the drug class identified from the presumptive testing. TLC requires minimal sample preparation, low cost, rapidity of analysis and simplicity. This method is purely employed to assist with correct choice of method for subsequent instrumental analysis.

1..2.2 Gas Chromatography

Gas Liquid Chromatography-Mass Spectrometry (GC-MS) is a powerful, inexpensive and easy-to-use analytical tool. Samples to be analysed are injected into an inert gas stream and swept into a tube packed with a solid support coated with a resolving liquid phase. The activity of adsorption between the components in the gas stream and the coating leads to a separation of the components in the mixture which are eluted into a mass spectrometer. The use of a mass spectrometer assists with compound identification in addition to quantitation. GC has its drawbacks such as the requirement for volatile compounds (37-39).

Gough and Baker (1981) highlighted problems around absorption and thermal instability around the direct analysis of heroin by GC. Several columns have been compared with each containing the same solid support coated with another stationary phase (40). Their findings concluded that some stationary phases were not suited for the analysis of heroin because of improper adsorption to the stationary phase. Their study left a conclusion that direct analysis of heroin using GC is connected with number of problems such as absorption, trans-

esterification, and the influence of other substances as well as the form in which heroin occurs (41-44). Nevertheless, due to its speed of analysis and high resolution, capillary GC is the most applied chromatographic technique used for such analysis.

Opiate drugs will chromatograph in both derivatised and underivatized form. Usually, in underivatized drugs, free hydroxide moieties are present in the form of 6-O monoacetylmorphine, morphine and codeine. These form hydrogen bonds with the analyte molecules and adsorb strongly onto various components of the GC system (44,45). These hydrogen bonds are sufficiently strong that they cause problems such as tailing of the compounds and, as a result of this, derivatisation of heroin is commonly employed. Derivatisation is also used to prevent the phenomenon of trans-esterification with one of the most common adulterants, paracetamol, by protecting the reactive groups from the heroin molecule. It also increases or decreases the analyte's volatility, improves separation or detection, or prevents thermal breakdown of the analyte. Derivatisation of heroin is most commonly achieved through the use of N, O- bis (trimethylsilyl) acetamide. A standard temperature programme program is used to separate the analytes, which will be identified using a Mass Selective detector. Identification is based on two pieces of information, namely retention time and mass spectral data. Each component of the drug is compared to the standards. For a derivatised sample the mass spectra should be compared to its derivatised standards (42,43,46).

1..2.3 High Performance Liquid Chromatography

Quantification of heroin is carried out using either GC or HPLC. As highlighted in the previous section, samples for GC are often derivatised and it works on the assumption that the sample has been completely and quantitatively derivatised. Derivatisation adds additional steps to the analysis, which can result in sample breakdown and contamination. Due to these reasons, most laboratories carry out qualitative analysis using GC-MS and then quantify the samples by HPLC (40).

HPLC overcomes a number of GC related problems such as absorption, heat instability and trans-esterification. No extensive derivatisation of samples is required which results in more reproducible data for comparison purposes. For the purpose of quantification of heroin by

HPLC, the baseline resolution of the compound must be achieved in the chromatographic analysis, thus a peak height or area can be assigned to one compound alone. It is also crucial to produce a calibration curve of the analyte using the same solvents in which the samples are analysed. This is particularly important, as small differences in pH can lead to different extinction coefficients when measuring UV absorption, which leads to inaccuracies in the quantification process. This technique has its limitations, which include lesser resolution and high solvent consumption compared to GC (40,46). In comparison to these current methods, XRPD holds an advantage, as no sample pre-treatment is necessary.

1.2.4 X-Ray Powder Diffraction

Literature reviews show a number of studies have been carried out in regard to drug analysis using XRPD. However, the use of XRPD as a field test and to be utilised in environment such as Airport, Border Control as a means to gather intelligence and IDQ simultaneously is yet to be fully explored. In 2015, an article reviewed the use of XRD in pharmaceutical environment to provide key information on the use of this technique to obtain data on crystal structure, detection of impurities, crystal morphology of active ingredients and to monitor batch or dosage uniformity. Samples were analysed using the new Bruker diffractometer to illustrate the dynamic use of XRD such as to identify drug substance forms, amorphous formulation (47). The aim of this study was to educate and demonstrate that XRD can be used as a stand-alone technique and can be used with other techniques such as Raman Spectroscopy and Fourier Transform Infrared Resonance.

A study in quantitative phase analysis by Rietveld methods for forensic science explored the use of Rietveld quantitative analysis to obtain valuable information which can be used for the purpose of material evidence analysis. Diffraction data's were analysed using a diffraction software MAUD. It was highlighted that the quality of the diffraction pattern can influence the quantitative phase analysis. Analysis of synthetic mixtures produced precise results with an absolute error below 2%. The methods uses the whole pattern fitting therefore it is less susceptible to variables such as preferred orientation. It has been reported in a recent study (48) the importance and advantages of XRPD in Forensic Science. Although it has been used widely in the pharmaceutical industry (49), this technique hasn't been used much in the field of Forensic drug analysis. This study looked into the use of XRPD in the analysis of drugs,

namely new psychoactive substances. Seized samples of heroin, cocaine and five new psychoactive substances were analysed using X-ray Powder Diffraction, Raman Spectroscopy and Infrared Spectroscopy. It was concluded that all of the new psychoactive substances and other illicit drugs were positively identified providing a reliable identification of the components.

1.3 X-Ray Spectroscopy

X-rays are electromagnetic radiation of wavelength about 1\AA , which is about the same size as an atom. X-ray is found to be in the portion of the electromagnetic spectrum between gamma rays and the ultraviolet. The discovery of X-rays in 1895 assisted scientists to probe crystalline structure at the atomic level. The use of X-ray diffraction was for the fingerprint characterisation of crystalline materials and the determination of structures. Each crystalline solid has its unique characteristic X-ray powder pattern, which may be used for its identification. It is often usual that when the material is identified, X-ray crystallography may be used to determine its structure (50,51). This includes information about how the atoms are packed together in the crystalline state and what the interatomic distance and angle are. X-ray diffraction is one of the important characterisation tools used in solid-state chemistry and materials science, which leads to determining the size and the shape of the unit cell for any compound. Diffraction experiments are also used for amorphous materials even though their pattern lack sharp diffraction peaks. In addition to this, diffraction data can be used to refine the lattice parameters of a crystal structure (52). There is a direct relationship between the lattice parameters and peak-shift. Therefore it is vital to refine the lattice parameter to increase the accuracy in reproducibility of the peak-shift.

The position of the diffraction peaks are determined by the distances between parallel planes of atoms. Bragg's equation predicts when diffraction actually takes place. The Bragg's Law $n\lambda = 2d_{hkl} \sin \theta$ where the wavelength (λ) is fixed, d_{hkl} is the interplanar spacing between two reflecting planes in a crystal and θ is the angle of incidence.

The Bragg's law is related to the wavelength of electromagnetic radiation and the diffraction angle and the lattice spacing in a crystalline sample. These diffracted X-rays are detected, processed and counted.

Diffraction is a prearranged event where three parameters are considered: the wavelength of the X-rays, the crystal orientation as defined by the angle θ and the d spacing of the crystal planes under consideration. For a given wavelength and set of planes one can conspire to arrange for diffraction to occur by continuously changing the orientation thus changing θ until a point arrives when Bragg's Law

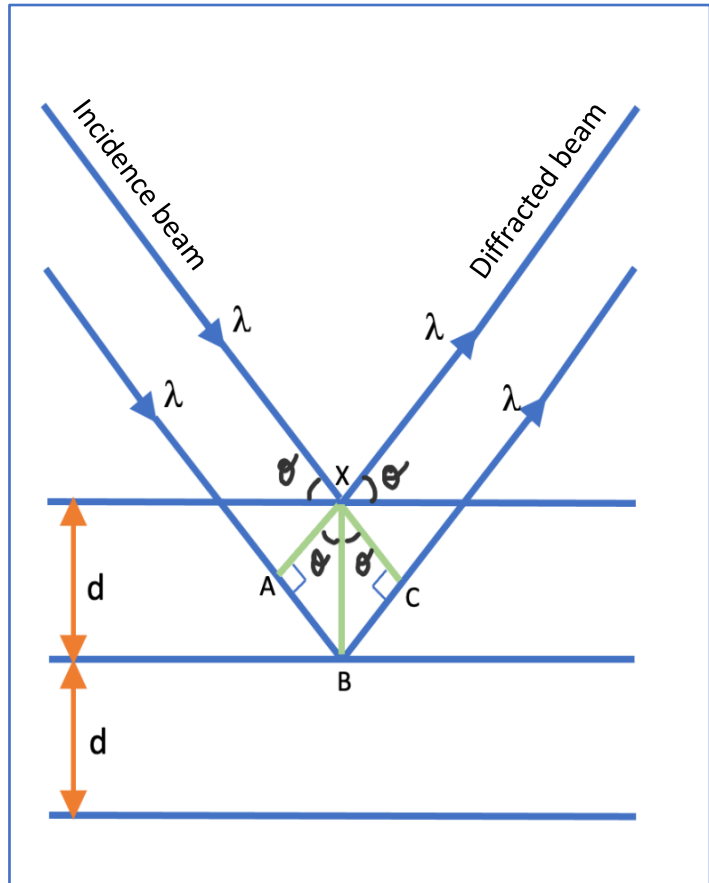


Figure 2 Schematic diagram displaying Bragg's law.

is satisfied and this is precisely when diffraction occurs (31,45).

To illustrate this, consider a crystal with lattice planar distances (d) where the beams are parallel to each other until it reach point X and at this point the beam strikes the surface and travel upwards. Similarly at point B the second beam scatters. It can be deduced that AB+BC is the distance travelled by the second beam, see Figure 2. The path difference between two reflecting rays is equal to an integer number of the wavelength. When monochromatic X-rays are incident upon a crystal, atoms in different layers act as a source of scattering radiation of the same wavelength. If Bragg's law is not satisfied, then the interference will be nonconstructive resulting in a very low-intensity diffracted beam (53).

1..3.1 Analysis modes

The most common analysis mode, reflection mode, where the divergent and diffracted beams are focused at a fixed radius from the sample position (θ - 2θ) with a fixed X-ray tube where the detector and source are located at the intersection points of the fixed radius (goniometer). This geometry allows the use of a divergent X-ray beam from a sealed tube without monochromatisation or parallelisation thus avoiding the loss of intensity (53,54). Variation of the Bragg-Brentano geometry has been used commonly used for phase analysis using powder diffraction instruments. This setup provides higher measurement speed, no powder spillage at high angles, provides a higher resolution with high intensity and has the capacity to analyse bulk samples. However, this mode can trigger sample displacement and transparency errors, cannot be used to analyse small samples.

Transmission mode, an alternative to reflection mode that preferred for the analysis of samples with lower absorbance properties, is where the x-ray pass through an x-ray transparent sample. This can be prepared in a glass capillary, between foils or thin solid sample adequate enough for X-rays. A focus beam or a parallel beam can be utilised. This is measured through the sample, suitable for samples which interacts weakly with x-rays. This setup employs a single detector and various soller slits to define the incident and scattered beam directions (55,56). This allows for the sample to rotate around its axis and avoids non-randomness of the powder sample i.e. preferred orientation. It can be used to measure small sample quantities, good measurement resolution hence slower measurement speed

1..3.2 Quantitative data analysis - Rietveld refinement

The Rietveld refinement method was developed by Hugo Rietveld in late 1960's and it was first reported at the seventh congress of the International Union of Crystallography in 1966. A mixture of two or more substances gives a diffraction pattern made up of the superimposed patterns of the individuals components. The intensities of the individual patterns are proportional to the concentrations of the phases present. Hence by measuring the intensities of patterns, the relative amounts of each phase can be determined. Rietveld generates calculated diffraction pattern which is compared with observed data. Least squares

regression is used to minimise the differences between the complete observed and calculated data (49).

1.3.3 Beam damage

X-ray exposure can cause alteration or structural damage to the organic crystals. This causes chemical bonds to break and change the structure of the specimen. Other forms of damages includes hydrocarbon contamination and heating of the sample. A study conducted to observe the importance of understanding the effects of X-ray exposure on small molecular crystals concluded that radiation induced changes were observed. The results also highlighted the importance of choosing the best experimental setup and parameters (57,58).

1.3.4 Amorphous solids

Amorphous solids are non-crystalline materials in which the atoms and molecules are not organised in a definite lattice pattern. Examples of such materials include glass, plastic and gel (36,47,59).

In a mixture of crystalline and amorphous phases, the crystalline and amorphous fractions can be estimated in two ways.

The crystalline fraction may be obtained by quantification of the individual crystalline phases with the use of appropriate standard substances. The amorphous fraction is then deduced indirectly by difference

When amorphous and crystalline fractions do not differ in their elemental composition but only in ordering, the ratio of the integrated intensities of the crystalline fraction to the integrated intensities of the amorphous halos can be used to compare the crystallinity of the otherwise similar materials or to calculate a value of crystallinity according to a more complex procedure. (60,61).

1.4 Chemical impurity profiling

Chemical profiling of seized synthetic illicit drugs has become one of the most important parts of strategic forensic investigation as the profile of an illicit drug sample provides information at several levels. It can be used to determine links between two or more samples. Comparison of drugs can be divided into several levels and it can be used to determine links between two

or more samples. Purity is one of several parameters used for profiling and to establish relationships between sample groups (35,62). More often profiling of drugs is based on the analysis of manufacturing impurities and by-products. This is carried out using different chromatographic methods that have been examined and published by many researchers.

Profiling of drugs includes, in addition to chemical analysis, another interdependent step, the interpretation and handling of the data. After chemical profiling the classification, i.e. grouping is commonly achieved using statistical analysis such as cluster analysis. Profiling results typically falls into 3 categories (i) identical, (ii) completely or in between (i) and (ii). For example, similar impurity profile indicates a link between the samples. Alternatively, samples having different profiles clearly do not belong to the same batch and this could be due to differences in starting materials or the production methods (35,63,64).

An inter-laboratory development of heroin profile method was carried out a study to develop a harmonised profile method and improve the interpretation for the resulting database of the chemical profiles using a relatively simple sample preparation without derivatisation (14). The results showed that the GC-FID system seemed to be stable and the intra-laboratory repeatability and reproducibility were acceptable. However, poor reproducibility at an inter-laboratory level was obtained. In conclusion, this study reported that a database for heroin comparison should be collected in a central laboratory instead of profiling in many laboratory. It was also concluded that this method should be used in conjunction with another major component analysis.

Another chemical profiling study compared nine illicit heroin samples by specifically looking at 18 impurity peaks. The variation between profiles was obtained by visual comparison however, this may not be used for court testimony as quantitation of selected impurities could be a necessity (59). In another experiment, toluene was used as an extraction solvent. The chromatograms were compared visually and highly specific profiles of heroin from four different origins were obtained. Different profiles from different geographical regions were compared based on the main alkaloids and adulterants from Johnston and King. The results were presented with the support of statistical analysis. The analysis results of classification were correct in over 83% however, it was concluded that the chemical composition of seized heroin changes over time, which may lead to misclassification (65).

In addition to GC methods, HPLC have been used in heroin profiling (66). Chromatograms of 24 illicit samples were compared visually. Moreover, percentages of diamorphine, acetylcodeine, noscapine, papaverine and few impurities were determined. Similarities between 33 street samples have also been determined without chemical impurity profiling (67). Headspace-gas chromatography (HS-GC) was used to determine residual solvent quantities. Heroin content and adulterants were obtained by GC and more information from diluents by HPLC.

Chemical profiling of complex samples has traditionally been based on GC analysis of impurities. Seized drugs usually have a complex composition making automatic profiling difficult. There are two major prerequisites for successful automated comparison (i) high resolution of the compound of interest and (ii) automated identification of impurity of peaks, typically based on the use of a highly selective MS detector or retention index (RI) monitoring techniques (68).

Profiling and analysing a suspected heroin sample simultaneously would add valuable scientific information to support law enforcement intelligence gathering and operational work. Identification of the components within various seizures can provide a wealth of information, for example, trends in usage of particular drugs, changes in diluents or adulterants and its purity. This research could provide a major advance in profiling and analysing suspected heroin samples using a rapid, non-destructive method. XRPD has the potential to play a pivotal role in unravelling the history of a given heroin sample's manufacturing and trafficking route (14,69,70). Sources of characteristic impurities found within seized samples may include:

1. The adulterants and cutting agents intentionally added to the mixture during production to dilute the drug. These chemicals mimic the drug itself.
2. Opium alkaloids. These are usually co-extracted during drug production but may not be completely removed from the end product.
3. By-products generated during drug manufacture, such as calcium carbonate and calcium chloride;

4. Precursor compounds, such as acetyl anhydride, and solvents used in drug manufacture are ingredients specifically incorporate its molecular structure into an illicit substance. For example, acetic anhydride most commonly used as a precursor for heroin manufacture (70).
5. Reagents are the ingredients required within a reaction to modify the precursor's molecule structure into a required substance.
6. Solvents are added to the mixture dissolving precursors and reagents to drive the chemical reaction, diluting the mixtures as well as separating and purifying other chemicals that are present (71).

Analysis of forensic casework seizures requires a careful, well thought out approach to the analytical sequence in order to maximise the obtainable information; thus XRPD is one of the techniques that should be considered more as a first line of attack. The current protocol for analysing bulk samples includes: physical description, presumptive testing, followed by Gas Chromatography Mass Spectrometry (GC-MS) and High Performance Liquid Chromatography (HPLC). XRPD is a non-destructive method of analysis for crystalline materials and would possibly be able to substitute current methods of analysis (24,26,37,72).

2. Objective of the study

The aim of this study is to demonstrate that X-Ray Powder Diffractometry can be used as a non-destructive technique for qualitative and quantitative analysis of known physical mixtures mimicking heroin samples.

The overall objectives of this pilot study includes:

1. Development of a method to enable qualitative analysis of known physical mixtures by X-Ray Powder Diffraction.
2. Optimisation of the instrumental parameters to enable quantitative analysis.
3. Explore and optimise the quantitative capabilities of Rietveld refinement on the data obtained.

3. Method

A Bruker D8 Advance X-ray diffractometer was used to collect the data for this study. The parameters used throughout the study are listed in the Table 2 below. The Bruker AXS Measurement Suite, Diffrac.EVA and Crystal Impact Match! were the software programs used for the analysis, to interpret the data and compare spectra, respectively. Corundum was used to calibrate the diffractometer and this is a crucial part to prevent 'tube drift' of the diffractometer. The peak position is recorded to monitor any change in tube intensity.

Table 2 Bruker XRD instrument setting-

Parameter	Reflection	Transmission
Geometry	Bragg-Brentano	Debye-Scherrer
Detector	LynxEye	LynxEye
Scan Type	Coupled Two Theta/Theta	Offset coupled two theta
Scan Mode	Continuous PSD Fast	Continuous Scan
Radiation	Cu-K α	Cu-K α
Generator	Current: 30kV Voltage: 10 mA	Current: 30kV Voltage: 10 mA
Primary Divergence Slit	Fixed	No slit
Axial Sollar Slit	2.5°	2.5°
Receiving Slit	0.6mm	0.6mm
Kβ- Filter	Ni-LowBeta	No Filter
Motorised slit	Primary motorised slit 0.3° Secondary motorised slit 3.0°	Global mirror

3..1 Beam damage

This experiment was carried out to observe any change in the diffraction pattern under the following condition: repeat analysis of the same sample.

Paracetamol samples were evenly spread onto a keptone film to create a sandwich layer supported by two slides. The sample in the film was then loaded onto a transmission holder for analysis Transmission. A total of 5 repeats were conducted without physically removing the samples from the auto sampler.

Instrumental parameter for the analysis: The X-Ray powder diffractometer patterns were recorded by mounting ~0.5mg of ground sample onto the transmission holder then exposing it to the X-Ray beam which is Cu K (α) radiation. The samples were analysed with the angular range of 10° to 60° using increment size of 0.020° for 96 minutes.

Paracetamol samples were loaded onto the PMMA sample holder to create a compact powder and this was evenly distributed out using a microscopic slide to evenly spread the sample.

3..2 Sample preparation

Various sample preparation methods were explored to determine which method would give the best quality of XRD spectra. The individual preparation experiments are listed in Table 2:

Chemicals used:

- Corundum-
- Paracetamol-
- Caffeine-
- Codeine-
- Sucrose-

Table 3 sample preparation used in this study

Sample preparation type	Preparation method	Analysis method	Type of analysis
Use of a mortar and pestle to grind the powder into the PMMA sample holder to create a compact powder	1g of physically mixed sample including the internal standard Corundum was ground using motor & pestle for approximately 1 minute. The ground sample was then transferred onto a sample holder and a microscope slide was used to evenly pack the holder and to create a smooth top layer.	Reflection	Qualitative and quantitative using known physical mixtures using internal standard.
Place loose powder on the polymethylmethacrylate (PMMA) sample holder-cavity diameter 25 mm and 1 mm depth	1g of physically mixed sample was transferred onto a reflection sample holder. The mixture wasn't ground.	Reflection	Beam damage, Qualitative and quantitative of internal standard.
Use of a mortar and pestle to grind the powder into the	Approximately 0.5mg of physically mixed sample was evenly spread onto a keptone film to create a sandwich layer. The sample in the film was then	Transmissi on	Method optimisation for known physical mixtures.

Transmission holder	loaded onto a transmission holder for analysis		
----------------------------	--	--	--

3.3 Transmission analysis method development

With a constant sample volume in the beam, the transmission mode provides reliable intensities over the full 2θ while the reflection setup could yield false intensities up to at least 10° . Line broadening for weak absorbing particles can be avoided and the statistical distribution of the particles in a capillary yields a diffraction pattern less affected by the effects of preferred orientation.

The following physical mixtures were prepared using pure phase chemicals using ratios. Each sample was analysed 3 times:

- * P50Ca50_1_BH_T1A2I2
- * P50Ca50_1_BH_T1A3I3
- * P50Ca50_1_BH_T1A4I4
- * P50Ca50_1_BH_T1A5I5
- * P50Ca50_1_BH_T2A3I3
- * P50Ca50_1_BH_T2A4I4_0.6mm
- * P50Ca50_1_BH_T2A5I5_0.6mm
- * P50Ca50_1_BH_T3A1I1_0.6mm
- * P50Ca50_1_BH_T3A2I2_0.6mm
- * P50Ca50_1_BH_T6A2I2
- * P50Co50_1_BH_T1A1I1_0.6mm
- * P50Co50_1_T2A1I1_060416
- * P50Co50_1_BH_T2A4I4_0.6mm
- * P50Co50_1_BH_T2A5I5_0.6mm
- * P50Co50_1_BH_T3A1I1_0.6mm
- * P50Co50_1_BH_T3A2I2_0.6mm
- * P33.3Ca33.3S33.3_1_BH_T1A1I1_0.6mm

- *P33.3Ca33.3S33.3_1_BH_T3A1I1_0.6mm
- * P33.3Ca33.3S33.3_1_BH_T2A4I4_0.6mm
- * P33.3Ca33.3S33.3_1_BH_T3A2I2_0.6mm

To find a suitable transmission method to analyse the physical mixtures 50:50 Paracetamol:Caffeine was analysed using the following parameters were changed: Time (**T**) of the analysis, Angular range ($^{\circ}$)(**A**) and Increment size ($^{\circ}$)(**I**). See Table 3.

Table 4 Analysis method used for transmission method optimisation

Method key	Instrumental parameter		
	Time (Minutes)	Angular Range ($^{\circ}$)	Increment Size ($^{\circ}$)
T1SA1I1	10mins	10-60 $^{\circ}$	0.020 $^{\circ}$
T1A2I2	10mins	10-60 $^{\circ}$	0.040 $^{\circ}$
T1A3I3	10mins	10-70 $^{\circ}$	0.060 $^{\circ}$
T1A4I4	10mins	10-80 $^{\circ}$	0.080 $^{\circ}$
T1A5I5	10mins	10-90 $^{\circ}$	0.10 $^{\circ}$
T2A1I1	20mins	5-60 $^{\circ}$	0.020 $^{\circ}$
T2A2I2	20mins	10-60 $^{\circ}$	0.040 $^{\circ}$
T2A3I3	20mins	10-70 $^{\circ}$	0.060 $^{\circ}$
T2A4I4	20mins	10-80 $^{\circ}$	0.080 $^{\circ}$
T2A5I5	20mins	10-90 $^{\circ}$	0.10 $^{\circ}$
T3A1I1	30mins	5-60 $^{\circ}$	0.10 $^{\circ}$
T3A2I2	30mins	10-60 $^{\circ}$	0.020 $^{\circ}$

3..3.1 Optimisation of slit

The following samples were analysed using the 0.2mm and 0.6mm sollar slit to observe any change peak position and intensity.

Samples	Slit size	Mode of analysis	Method- Angular range: Increment Size: Time
Paracetamol 100%	0.6mm, 0.2mm	Reflection	5-40°, 0.020°, 1720, 96.00s
Caffeine 100%	0.6mm, 0.2mm	Reflection	5-40°, 0.020°, 1720, 96.00s
Codeine 100%	0.6mm, 0.2mm	Reflection	5-40°, 0.020°, 1720, 96.00s
Paracetamol 100%	0.6mm, 0.2mm	Transmission	5-70°, 0.020°, 1720, 96.00s

3..3.2 Optimisation of angular range, run length and increment size for reflection mode

To achieve the optimal condition needed for the analysis of physical mixtures, the following parameters in Table 4 were considered:

Table 5 Methods used for Reflection mode

	Method	Sample type
<i>Short run1</i>	8mins, 10-60°, 0.026°	Sample without internal standard, Sample with internal standard
<i>Short run2</i>	10mins, 10-60°, 0.020°	Sample without internal standard, Sample with internal standard
<i>Long run</i>	58mins, 10-80°, 0.0020°	Sample without internal standard, Sample with internal standard

The long run was used as a standard measure to compare against short run 1&2 methods. This was mainly to compare the peak positions and whole pattern fitting of the diffractogram between transmission and reflection mode.

3.4 Quantification using Rietveld refinement

CrystalDiffract Match software was used to carryout this analysis. The variables in the refinement can be separated into two groups: the first group is the structural parameters, including atom positions, occupancies and temperature and these factors determine the intensity of the peaks.

The analysis began by preparing the diffraction data for use in the refinement by defining reflection positions. Initial refinement is carried out on background parameter and overall scale factor. The lattice parameter and zero point correction are added to the refinement to fit the peak positions. Based on this results the profile parameters were also refined to counteract any poorly fitted peak positions (73,74). A visual comparison between the observed and calculated diffraction patterns also aided in identifying the parameters required to achieve convergence. R- factors and X^2 values were used to further inspect the fitting after changes to the parameters. The weight fractions of the individual phases were calculated from the refined parameters and the unit cell volumes calculated from reference structure files of the phases (74,75).

4. Results and Discussion

The reflection diffractogram (blue) and the transmission diffractogram (red) of paracetamol is displayed in Figure 3. The diffractograms obtained were compared against the user reference database created using structure files (.str and .cif) taken from the Cambridge Crystallographic Data Centre (CCDC) and the Crystallographic Open database (COD). The reflection data exhibits prominent sharp peaks indicating a good crystalline sample. In comparison to the transmission analysis, the reflection analysis provided fewer but more intense peaks, see Figure 3 and Figure 4. This is expected as the Bragg-Brentano geometry enables the use of a divergent X-ray beam without monochromatisation or parallelisation, resulting in higher intensity in comparison to transmission analysis (76). The reduction of the number of peaks in reflection analysis versus transmission analysis relate to the lower absorbing crystallites that do not reflect the divergent x-ray beam effectively (77).

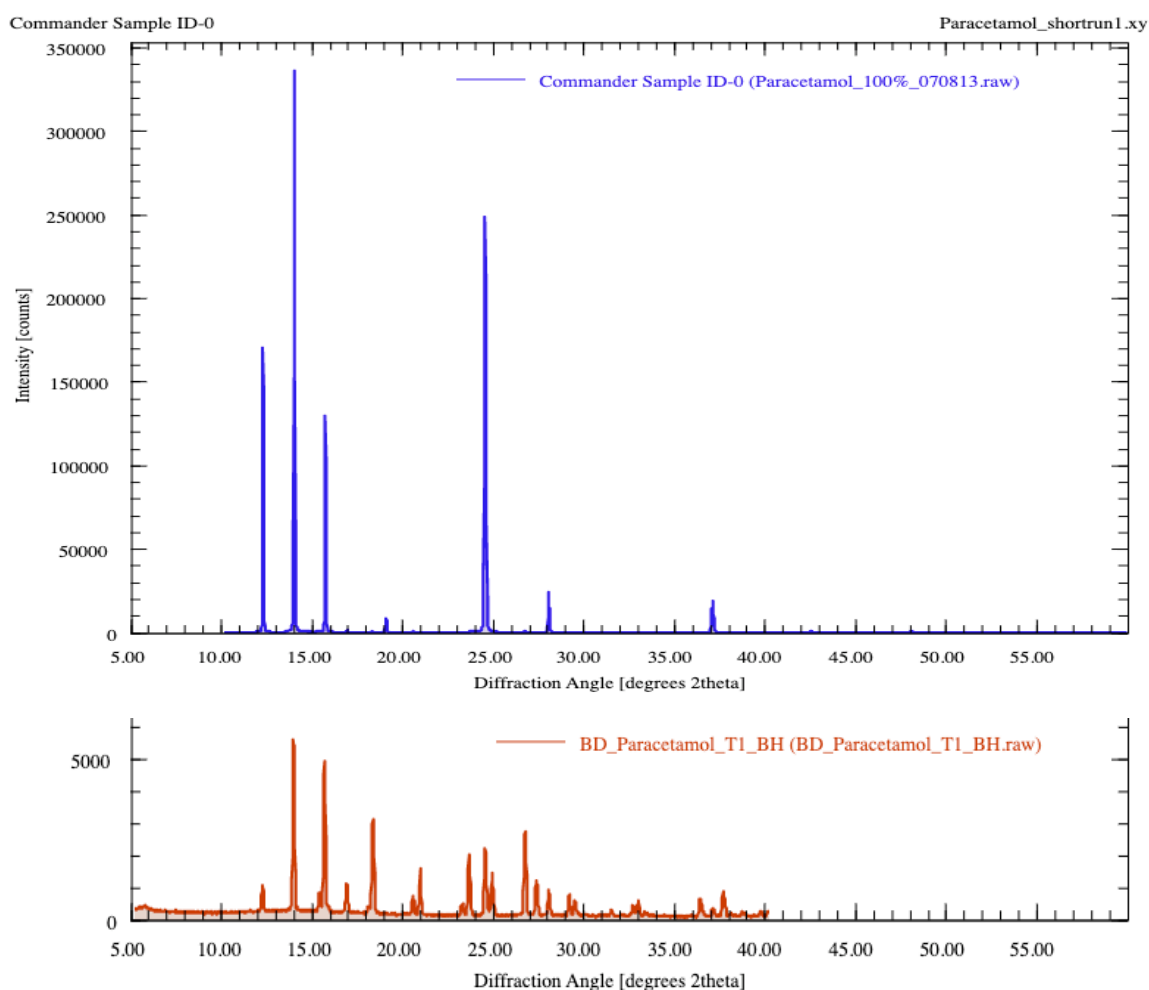


Figure 3- Pure phase of Paracetamol using Reflection and Transmission setup

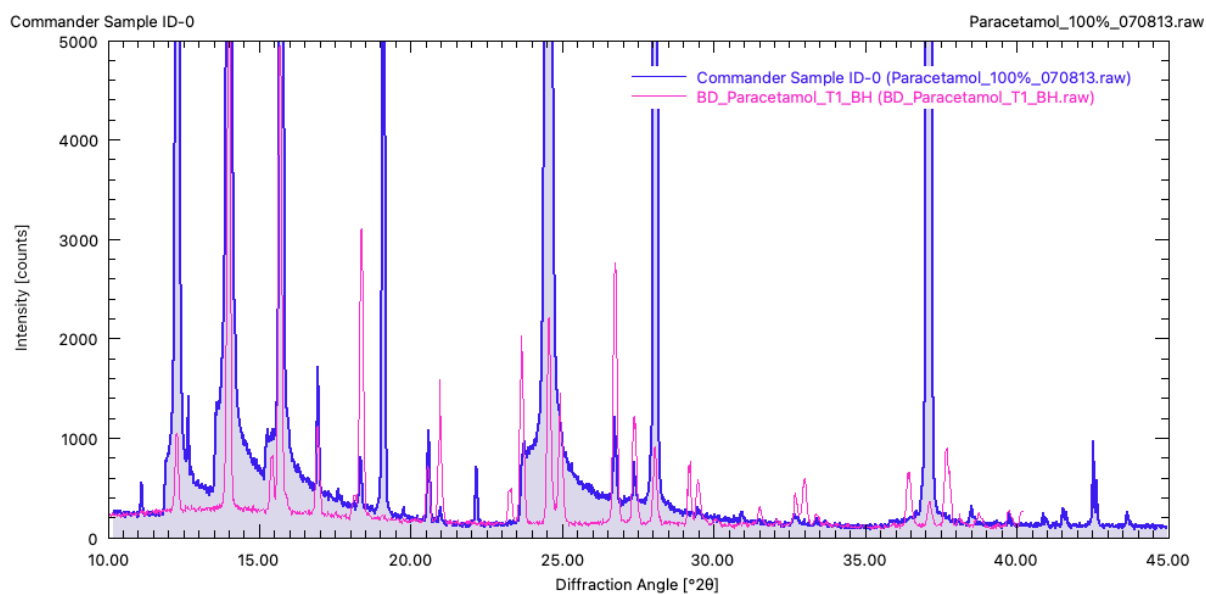


Figure 4 illustrates the differences in diffraction data for Paracetamol analysed using Reflection and Transmission mode.

4.1 Beam damage

Prolonged exposure to X-ray radiation is known to cause damage to the crystal structure. Studies published by (58,78) highlighted that beam damage can lead to major structural changes such as tilting, lattice expansion and an intensity reduction of the Bragg-Brentano reflection. There is a direct relationship between the lattice parameters and peak-shift. Therefore it is vital to minimise lattice expansion to increase the accuracy and reproducibility of the peak-shift (79).

As part of the method development the likelihood and extend of beam damage occurring during repeated analysis was investigated to understand the impact of beam damage on further optimisation of the analysis method. Table 6 displays the %-change of the most intense peaks ($\geq 25\%$ relative intensity) for paracetamol in transmission and reflection analysis and caffeine and codeine in reflection analysis only.

The data obtained from the beam damage experiment did not demonstrate any trendable change over the repeated analysis runs and it is observed that the intensity change observed from the reflection data is most likely due to instrument variability rather than beam damage. A percentage change $>10\%$, highlighted in bold in Table 6, was observed for paracetamol during transmission analysis only, which is likely due to the lower maximum signal intensity observed of 58.1 counts (transmission) and 39236 counts (reflection). The peak at 20.8°

appears to exhibit an intensity loss between 14 – 28%, highlighting that some beam damage could be occurring. But when looking inspecting the %-change over the 5 repeat runs it is noted that the peak reduction is greater in the first two repeat analysis highlighting between analysis variability making it impossible to accurately quantify the %-signal loss. The data displayed in Table 6 highlights that the variability observed within the beam damage experiments is not significant for the analysis time window investigated. This highlights that the same sample could be analysed repeatedly for the method optimisation activities.

Table 6 Comparison of the %-difference obtained for the main peaks of paracetamol, caffeine and codeine in repeated analysis..

Sample	Analysis mode	Angle (2θ)	Intensity (counts)	Repeat 1	Repeat 2	Repeat 3	Repeat 4	
Paracetamol	Transmission	13.8	58.1	1%	6%	5%	4%	
		15.5	51.4	-3%	-2%	1%	-3%	
		18.2	32.4	-4%	2%	-3%	6%	
		26.6	28.8	6%	6%	5%	5%	
		24.4	23.1	-1%	-2%	-1%	0%	
		23.5	21.1	-12%	-9%	-4%	-4%	
		20.8	16.5	-21%	-28%	-14%	-16%	
		24.7	15.1	-11%	-8%	-2%	-6%	
	Caffeine	Reflection	24.4	39236	1%	2%	1%	2%
			15.5	31345	-2%	-2%	-3%	-3%
			12.1	25421	0%	-1%	0%	0%
			18.2	24716	0%	1%	1%	-2%
			23.5	22476	-1%	-1%	-1%	-2%
			26.6	20197	1%	1%	-2%	-2%
20.4			17110	2%	-1%	-1%	-1%	
11.8			70989	1%	0%	0%	0%	
12.0			84955	0%	0%	-1%	0%	
26.4			28517	-1%	-2%	-2%	-2%	
Codeine	Reflection		27.1	30248	1%	0%	1%	-1%
			12.8	21073	-1%	-1%	-1%	-2%
			13.1	20779	0%	-1%	-1%	-1%
			13.4	28421	-1%	-1%	-2%	0%
		13.5	43673	-1%	-2%	-2%	-2%	
		16.7	15890	-1%	-2%	-2%	-1%	
		17.4	16438	0%	-1%	-2%	-1%	
		17.9	21228	0%	0%	-1%	0%	
		22.7	12328	-2%	-1%	-2%	-2%	
23.5		24836	0%	-1%	0%	-1%		

Figure 5 displays an overlay between paracetamol analysis run one and run five to visually highlight the differences observed within Table 6 that could have been caused by beam damage during the repeated analysis of the same sample in transmission mode. As visible in Figure 5, a slight decrease is observed in the peak with a corresponding 2theta of 20.8°. This could impact accurate quantitation as repeated X-ray's radiation could degrade the sample matrix. According to Glaeser.R, 2000(80) and Nave.C, 1995 (81) the beam places a strain on

the quality of the diffraction pattern as a set number of X-rays has to pass through the sample in a transmission mode to produce desired number of counts making up the diffraction peaks.

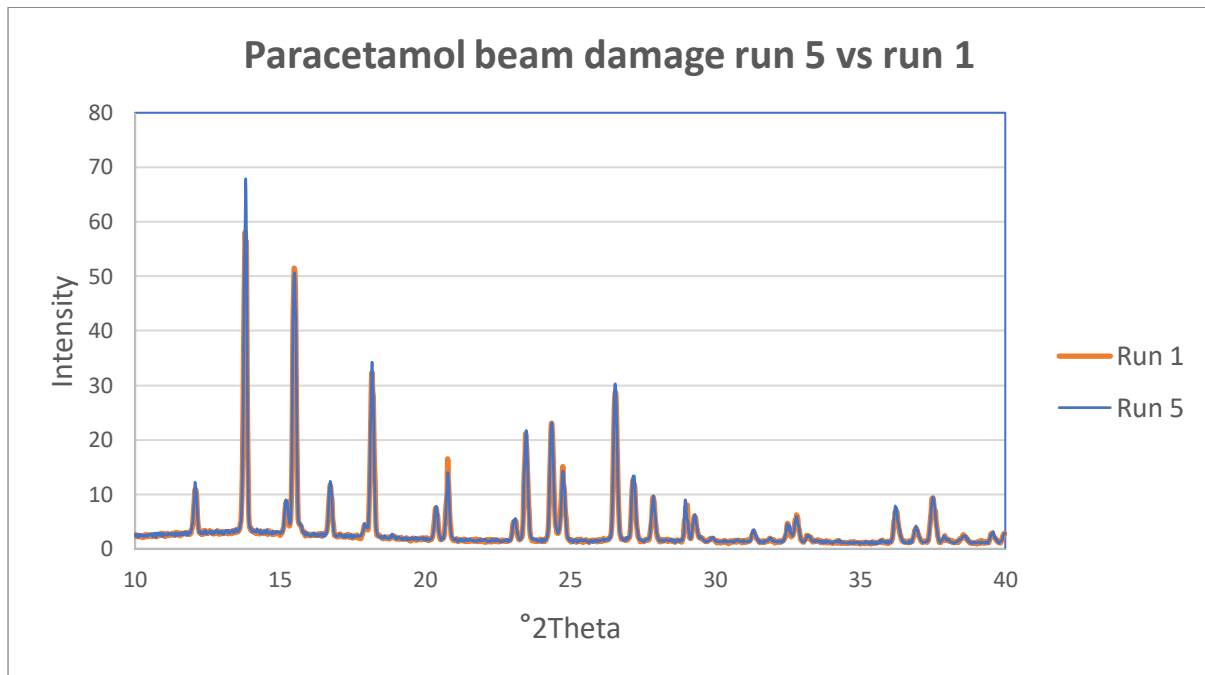


Figure 5 Comparison of damage between run 5 vs run 1 for Paracetamol

4.2 Sample preparation

Figure 6 displays a diffraction pattern of corundum ground, red trace, and non-ground, blue trace collected using reflection mode to assess the need for sample manipulation prior to analysis. The gold trace, displays the difference between the ground and non-ground diffractogram and highlights a minor difference in absolute peak intensities. Additionally, the peak shape of the ground corundum does exhibit slightly poorer peak shapes in comparison to the non-ground sample. The poorer peak shape could be due to the formation of microcrystals during the grinding process. Preparation of a sample is crucial in achieving a high quality data to avoid disproportionate crystallite orientations, insufficient number of crystallites in the sample and a representative intensity distribution for the sample. The ideal sample should provide a statistically infinite, randomly orientated crystallite no larger than 10 μm (82). Large crystallite sizes and non-random crystallite orientations both lead to peak intensity variation. According to Connolly, J., 2010 (83) the homogeneity of a complex sample needs to be maintained to obtain diffraction patterns from two or more phases that are not directly proportionate to the amounts of phases in the mixture.

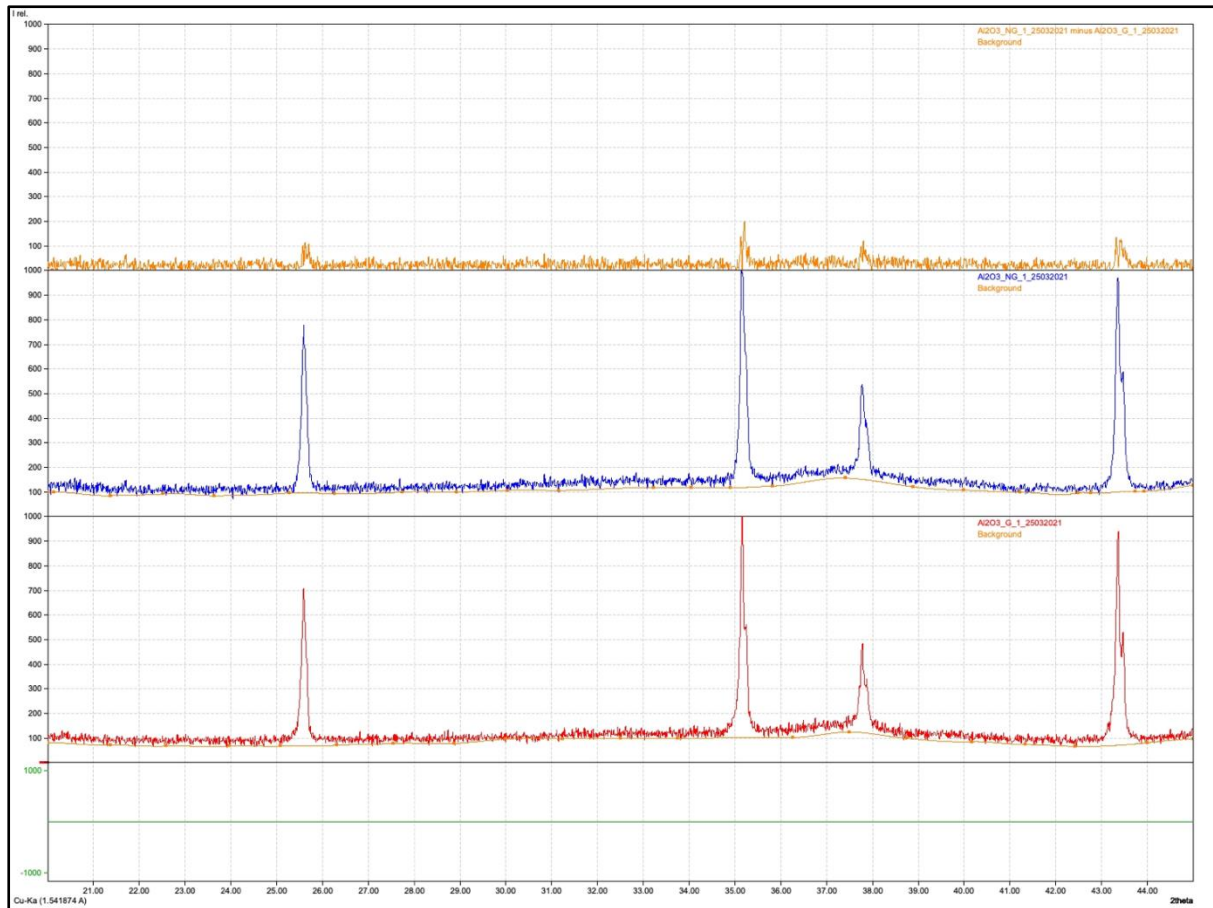


Figure 6 Comparison of ground Corundum (red trace), non-ground Corundum (blue trace) and difference between ground and non-ground Corundum (gold trace).

The approach to sample preparation is based on the sample's reactivity, hardness and behaviour of the phases. This needs to be considered before using an appropriate technique. In addition, this will have an effect on the quantification of the sample especially with Rietveld refinement due to potential peak intensity variations (73,84). Although the results below do not show any significant difference in ground and non-ground, this cannot be automatically applied to other pure phases in this study. For example, sucrose used in this study contained larger crystallite sizes $>10 \mu\text{m}$ therefore without some degree of sample preparation the measured diffraction pattern will not support the expected results from an ideal sample. Therefore, the samples were ground and prior to transferring into the well of the PMMA sample holder using the top-loading bulk powder for reflection analysis (50).

4.3 Transmission analysis method development

4.3.1 *Optimisation of slit*

The impact of changing the slit size was assessed for transmission analysis, see Figure 7. This figure compares the slit width of 0.2 mm, red trace, and 0.6 mm, blue trace, and the difference between both diffraction patterns is displayed in the green trace. A significant difference can be observed between the 0.6 mm slit and the 0.2 mm slit. The diffraction pattern of the 0.6 mm slit is more intense in comparison to the 0.2 mm slit pattern. This can be observed by the baseline noise in the red trace and the residual peaks in the green trace. Additionally, two peaks at a 2θ of 20.8° and 32.8° are not observed in the narrower, 0.2 mm slit diffraction pattern.

In order to obtain a precise diffraction data, the diffraction intensity needs to be enhanced, to minimise any diffraction broadening, peak shift, distortion and poor background. The slit width can affect the peak intensity, shape and position of the peak (50) therefore it is crucial to choose the best receiving slit to minimise errors caused. The slit dimensions can be optimised to improve quantitation by Rietveld Refinement as the use of a wider slit has been reported to provide a better diffraction pattern with increased intensities (5). Based on this knowledge Figure 7 shows better results using the 0.6mm receiving slit due to improved signal to noise (49).

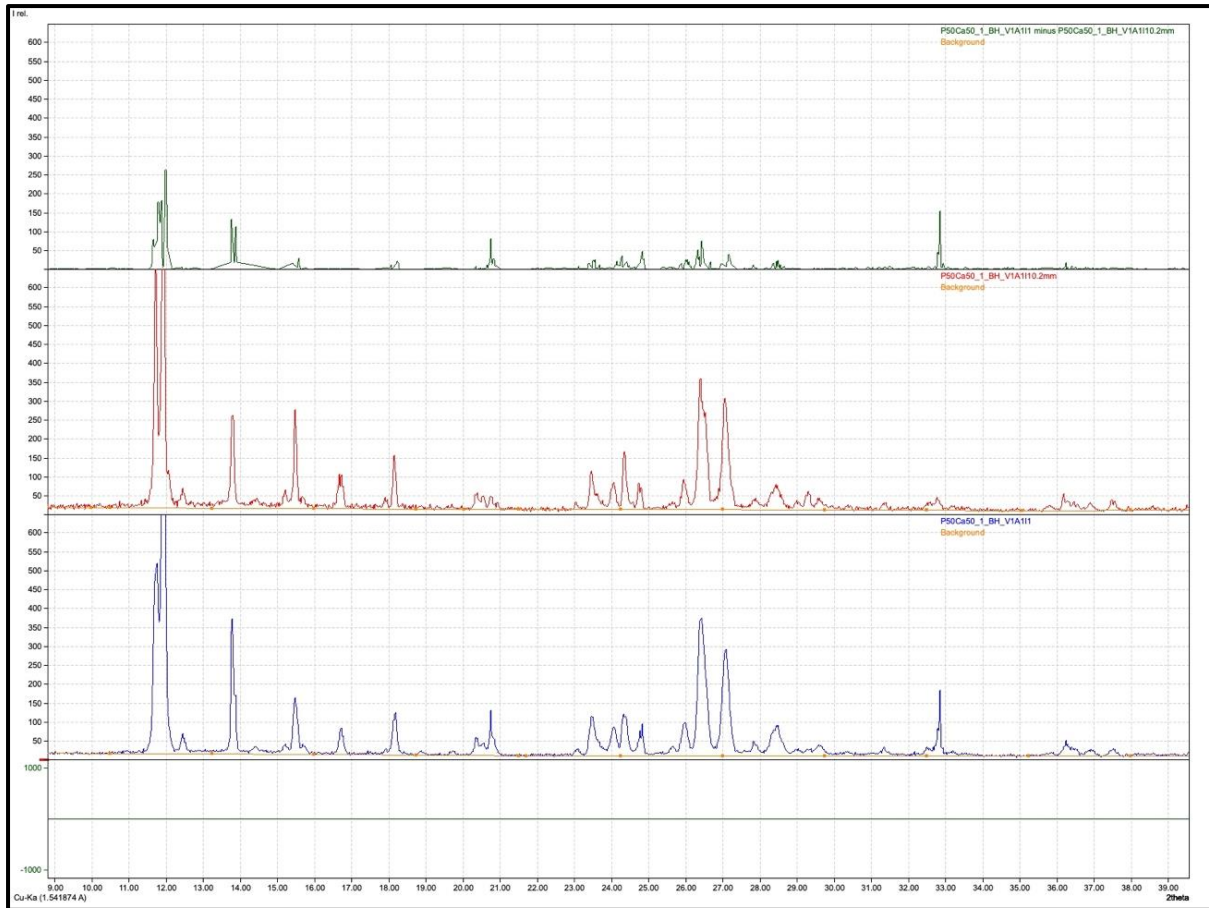


Figure 7 Comparison of a 50:50 caffeine:paracetamol physical mixture analysed using a 0.2mm slit size (red trace) and a 0.6mm slit size (blue trace). The green trace highlights the difference between the 0.2mm and 0.6mm slit diffractograms.

4.3.2 Optimisation of angular range, run length and increment size

The transmission analysis parameters were optimised to find the optimal angular range, total run time and the increment size. Figure 8 compares the diffraction pattern analysed for 10 minutes with an increment size of 0.020 and an angular range of 5-60° (orange) with a diffraction pattern analysed for 10 minutes, an increment size of 0.100 and angular range of 10-90° (blue). This highlights that no additional diffraction peaks were observed in the wider (between 60-90°) angular range (blue) diffraction pattern and thus a wider angular range is not required for the different mixtures assessed. Figure 8 does also display a diffraction pattern analysed for 20 minutes with an increment size 0.020 and an angular range of 5-60° (grey). When comparing this run against the others a clear difference can be observed in the peak intensity where the peaks in the grey trace (20 minute run time) are much more abundant than the peaks obtained during the 10 minute analysis. Figure 9 overlays the same

patterns but focusses on the peaks between 10 to 40° 2theta and highlights that all the peaks are more abundant when compared to the other runs. Thus an increase in overall analysis time does increase the peak intensity in the diffraction pattern. This is hypothesised to be related to the increased time spend for the data to be collected at each datapoint.

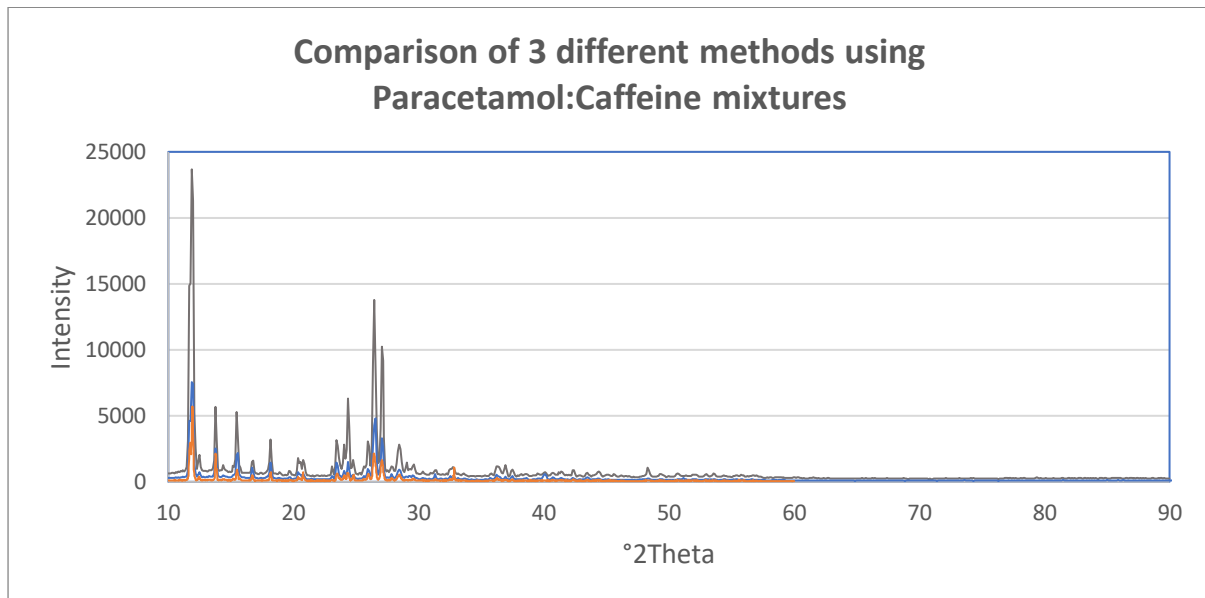


Figure 8 Transmission method optimisation for physical mixture ; Grey line = T2A5I5, Blue line = T1A5I5, Orange line= T1A1I1.

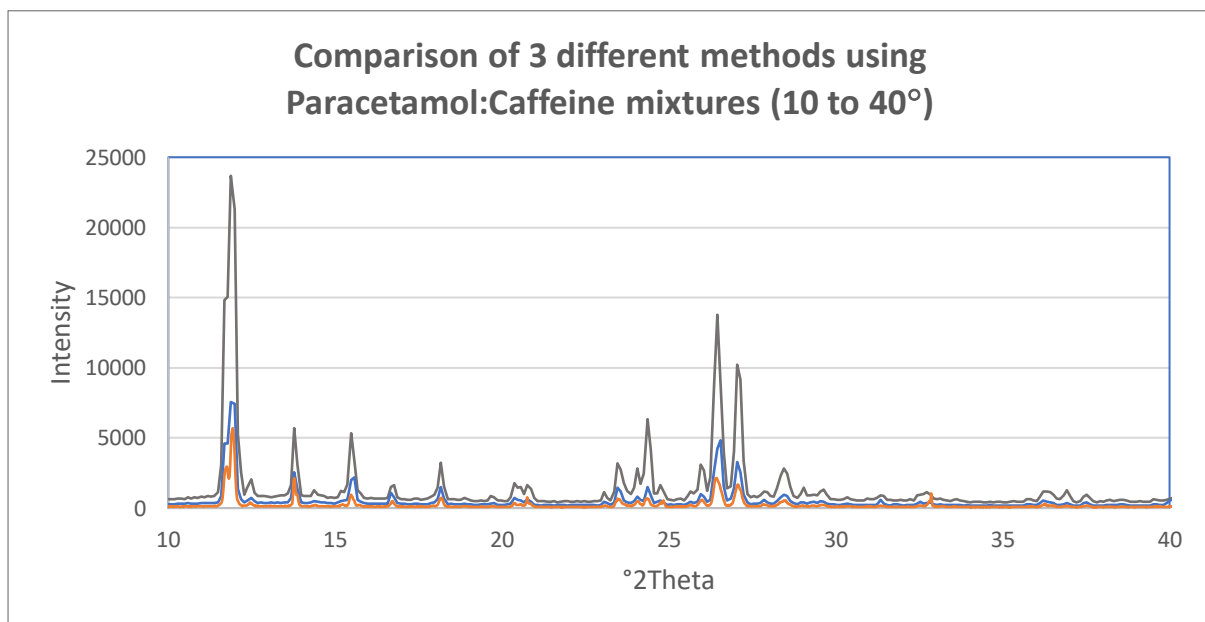


Figure 9 Transmission method optimisation for physical mixture zoomed between 10-40°; Grey line = T2A5I5, Blue line = T1A5I5, Orange line= T1A1I1.

In addition to an increase in peak intensity observed as a result of increasing the overall analysis time, Figure 9 also highlights a small increase associated with the change in increment size (blue vs orange). This increase in peak intensity is less prominent in comparison to that observed in the grey pattern but this highlights that the intensity increase in the grey pattern is likely due to the change in both increment size and overall runtime.

Figure 10 highlights impact of changing the angular range, run length and increment size on quantification. The bar chart displays the average difference between the actual % w/w and calculated % w/w for the 50:50 caffeine:paracetamol physical mixture analysed on the various increment sizes and runtimes. Additionally, the error bars highlight the 95% confidence interval obtained from the standard deviation of the three repeat analyses. The deviation between the actual and calculated amounts for all runs was between 0.04% and 7.5%. The chart highlights that the using a 0.020° increment size at an overall runtime of 20 minutes provided the most accurate and precise quantitative data in comparison to the other measurements based on the Rietveld refinement displayed in Figure 10. This combination provided an accuracy variation of 0.4% and a standard deviation of 0.06, which was the lowest observed.

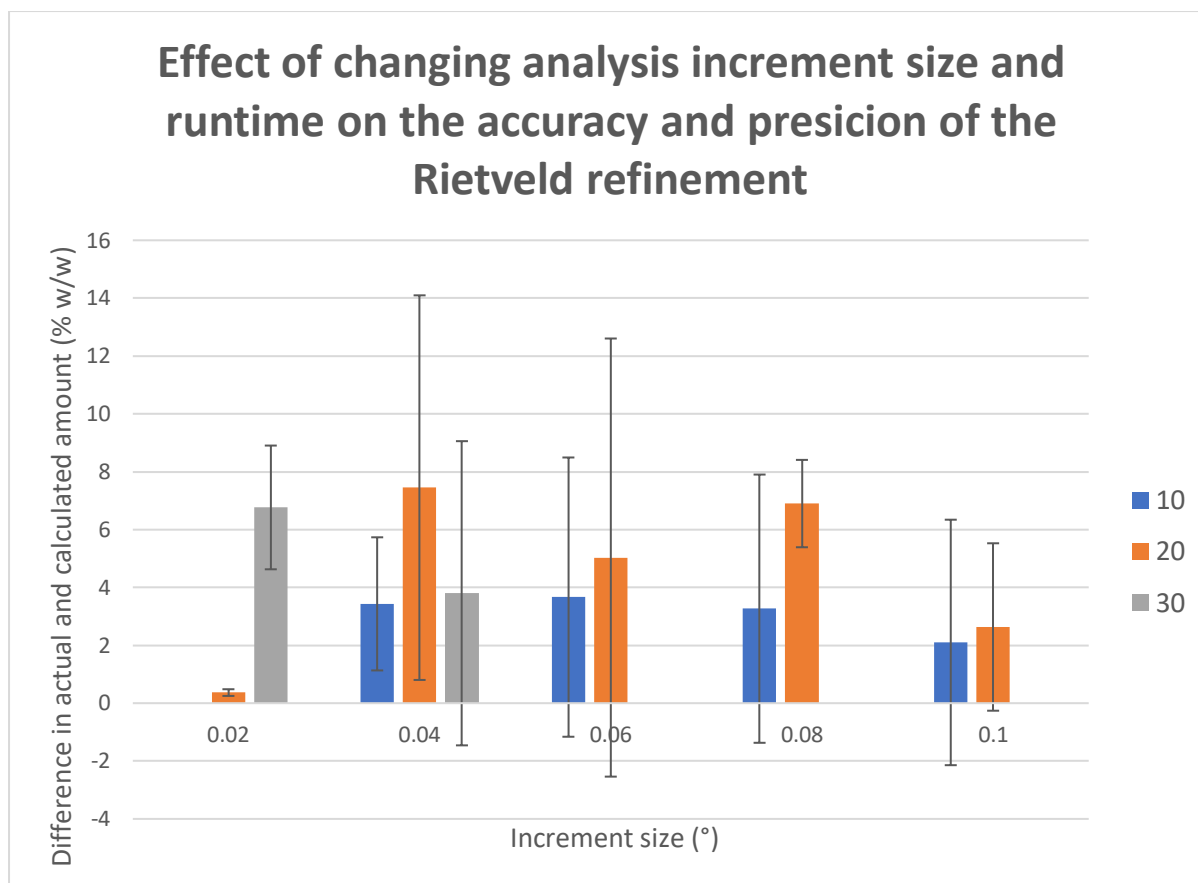


Figure 10 Effect of changing analysis increment size and runtime on the accuracy and precision of the Rietveld refinement

4.4 Quantification using Rietveld refinement

The quantitative capability of the Rietveld refinement on more complex mixtures at a variety of different ratios was assessed. Table 7 displays the accuracy and repeatability of the Rietveld refinement for caffeine, corundum and paracetamol by displaying the actual amount, average calculated amount and relative standard deviation of the replicate analyses. For the different samples analysed, the amount of caffeine and paracetamol were varied whilst the amount of corundum was kept the same. The actual quantities of the mixtures analysed can be found in column three and the calculated amount including its 95% confidence interval is displayed in column four, the relative standard deviation of the calculated amount is displayed in column five of Table 7. The calculated amount of only four (highlighted in green) of the 12 sample component mixtures matched the actual amount of the physical mixtures prepared within the 95% confidence interval. This is not surprising as the relative standard deviation associated with these results is above 10%, hence their 95% confidence interval would not

have included the actual amount if the relative standard deviation was in line with the others displayed in Table 7. The absolute deviation in accuracy ranged from 1.5% up to 9.4% This is quite large especially if this procedure is to be used to quantify seized heroin samples. This deviation is also not suitable when compared to other analytical capability currently used for this purpose such as GC-MS or LC-MS, where an absolute deviation around 1 to 2% is more likely. The repeatability is also high when taking into account the levels of components to be quantified, these amounts are 10% or higher this would lead to an expectation for the relative standard deviation to be around 2 to 3% (in line with variability obtained using LC and GC analysis). This is only met in three of the 12 components and thus the methodology requires further optimisation or additional Rietveld refinement is required to allow for a better prediction improving the overall accuracy and precision. Alternatively, the use of an internal standard, corundum, could improve the quantitative predictions of the Rietveld refinement, see Table 8 showing Rietveld refinement data.

Table 7 data show quantification of samples with and without internal standard.

Sample	Component	Actual amount (% w/w)	Calculated amount (% w/w)	Relative standard deviation (%)
TS1_IS_1_30 032021_MR	Paracetamol	9.99	11.73 ± 5.66	24.13
	Caffeine	69.28	64.53 ± 3.74	2.90
	Corundum	20.73	23.73 ± 2.00	4.21
TS2_IS_1_30 032021_MR	Paracetamol	20.17	21.67 ± 6.31	14.56
	Caffeine	59.87	52.83 ± 0.99	0.94
	Corundum	19.96	25.50 ± 5.57	10.92
TS3_IS_1_30 032021_MR	Paracetamol	30.44	23.43 ± 3.13	6.68
	Caffeine	49.05	51.23 ± 1.68	1.64
	Corundum	20.51	25.33 ± 2.16	4.26
TS4_IS_1_30 032021_MR	Paracetamol	39.74	30.37 ± 2.53	4.17
	Caffeine	39.59	45.00 ± 4.33	4.81
	Corundum	20.67	24.67 ± 5.83	11.82

Table 8 displayed the quantification of paracetamol when corundum is used as the quantitative internal standard for the Rietveld refinement on the same data used for Table 7. Paracetamol was used in this situation to mimic the diamorphine component in a seized heroin sample to assess the quantitative capability of the Rietveld refinement method. In this situation paracetamol was correctly identified as a component in the mixture, which was quantified against the corundum internal standard rather than quantifying each individual component (including Caffeine) using the Rietveld refinement method. This mimics are more

representative real-world scenario as not all the impurities require quantification. The data obtained is displayed in Table 8. On a first glance it is noticeable that the calculated amount including its 95% confidence interval does contain the actual amount of paracetamol in the mixture, highlighted by its green colour. The absolute error for the quantification of paracetamol over a range from 10 to 50% w/w when using an internal standard was 1% or less, whilst the maximum relative standard deviation was 5.26%. A relative standard deviation of 5.26% at an absolute amount of 10% w/w equates to a variability of approximately 0.5% and is therefore deemed acceptable. The data displayed in Table 8 highlights that the use of XRPD provides suitable analytical data to allow for quantitative analysis using Rietveld refinement when a suitable internal standard is used.

Table 8 shows the quantification results obtained

Sample	Component	Actual amount (w/w)	Calculated amount (% w/w)	Relative standard deviation (%)
TS1_IS_1_30032021_MR	Paracetamol	12.60	11.60 ± 1.22	5.26%
TS2_IS_1_30032021_MR	Paracetamol	25.20	25.53 ± 1.67	3.27%
TS3_IS_1_30032021_MR	Paracetamol	38.29	37.43 ± 2.31	3.09%
TS4_IS_1_30032021_MR	Paracetamol	50.09	49.43 ± 0.70	0.71%

5. Conclusion

In conclusion, a suitable method was developed to analyse physical mixtures containing caffeine, codeine and paracetamol with and without the use of corundum as an internal standard using Bruker D8 Advance. This enabled qualitative analysis through a user database containing structure files of paracetamol, caffeine and codeine.

The qualitative method was optimised to enable successful quantitative analysis. Parameters investigated included a comparison between transmission and reflection, which showed that the latter provided higher peak intensity and more repeatable data. Other parameters that were optimised included, analysis time, angular range, increments size and slit width in addition to an assessment of the possibility of the X-ray's damaging the crystal structure (beam damage). It was noted that an increase of the analysis time, increased the peak intensity. This is preferred when performing whole pattern fitting such as Rietveld refinement due to increased signal to noise at the larger angles. The increment size and runtime were assessed and chosen based on the accuracy and repeatability of the quantitative data obtained following Rietveld refinement. A runtime of 20 minutes with an increment size of 0.020° provided an accuracy error of 0.4% with a standard deviation of 0.06 using a 50:50 caffeine:paracetamol mixture.

The change in angular range did not directly impact the qualitative and quantitative aspects of the data but this could have been as no peaks were observed above 60° . This could have been as a result of the physical mixtures used and the impact of this will need to be reassessed when illicit substances such as heroin. Data obtained using a slit width of 0.6mm provided better signal to noise in comparison to a 0.2mm slit. Finally, the possibility of beam damage was investigated through repeated analysis to ascertain its likelihood of occurring and impacting the method optimisation when using the sample. The data highlight that no significant different diffractograms were obtained following this experiment.

The quantitative capabilities of the Rietveld refinement were assessed via the identification and inclusion of all components present in the physical mixture. This highlighted high variability on repeated analysis of paracetamol, up to 24% RSD. However, when partial identification of the physical mixture was performed and normalised using an internal

standard, the data obtained was deemed highly accurate (calculated amount +/- 95% CI included actual amount) and precise (maximum RSD of 5.3%) over the investigated range of 12.6% w/w to 50.1% w/w. This approach mimics a forensic setting more closely through identification and quantification of the active ingredient. The use of an internal standard is however required to obtain accurate and repeatable data.

The data obtained highlights that X-Ray Powder Diffractometry can be as a non-destructive technique for qualitative and quantitative analysis of known physical mixtures containing caffeine, codeine and paracetamol mimicking heroin samples.

6. Further work

The main aim of this research is to develop a harmonised non- destructive method that will enable the analysis of street heroin. Using the data from this pilot study the next approach to this study should be focused on:

1. The effect of preferred orientation on a diffraction pattern
2. The presence of amorphous and polymorphs in an unknown sample and how this can be alleviated.
3. The use of different sample holders and sample preparation to find the most appropriate sample preparation and sample loading method
4. A robust and reliable method to analytically characterise and quantify seized heroin samples from different sources.

A sample holder which can be used at the crime scene to retrieve a small amount of suspected sample for XRPD analysis.

Publication of articles in peer-reviewed journals to exhibit the work carried out.

7. Bibliography

1. World Drug Report 2020 (United Nations publication, Sales No. E.20.XI.6).
2. European Monitoring Centre for Drugs and Drug Addiction (2020), European Drug Report 2020: Key Issues, Publications Office of the European Union, Luxembourg.
3. World Drug Report 2009 (United Nations Publication Sales No. E.09.XI.12).
4. Home Office. ANNUAL REPORT ON THE HOME OFFICE FORENSIC EARLY WARNING SYSTEM (FEWS) A SYSTEM TO IDENTIFY NEW PSYCHOACTIVE SUBSTANCES. 2012;(May).
5. Madsen IC, Hill RJ. Effect of divergence and receiving slit dimensions on peak profile parameters in Rietveld analysis of X-ray diffractometer data. Vol. 21, Journal of Applied Crystallography. 1988. p. 398–405.
6. Engel BS. Trends and Developments. Trust Trust [Internet]. 1996 Dec 1;3(1):3–3. Available from: <https://academic.oup.com/tandt/article-lookup/doi/10.1093/tandt/3.1.3>
7. DRUG STRATEGY 2010 Reducing Demand Restricting Supply Building Recovery: Supporting People to Live a Drug Free Life. 2010;1–26.
8. Cross-cutting issues: Evolving trends and new challenges [Internet]. 2020. Available from: www.unodc.org/wdr2020
9. Office for Health Improvement & Disparities. Adult substance misuse treatment statistics 2020 to 2021: report [Internet]. GOV.UK. 2021. Available from: <https://www.gov.uk/government/statistics/substance-misuse-treatment-for-adults-statistics-2020-to-2021/adult-substance-misuse-treatment-statistics-2020-to-2021-report> 2010. Available from: <https://www.unodc.org/documents/data-and-analysis/tocta/5.Heroin.pdf>
10. European Commission. Horizon 2020 - Work programme 2014-2015 Secure societies, Protecting freedom and security of Europe and its citizens. 2014;2015(March 2014).
11. Home Office. Drug Misuse Declared: Findings From the 2011/12 Crime Survey for England and Wales. 2012 [cited 2014 Oct 21]; Available from: <https://www.ncjrs.gov/App/AbstractDB/AbstractDBDetails.aspx?id=262261>

12. Haddad PR. The analysis of controlled substances. *TrAC Trends Anal Chem.* 2003;22(11):1.
13. CPS. Drug Offences | The Crown Prosecution Service [Internet]. *Cps.gov.uk*. 2019. Available from: <https://www.cps.gov.uk/legal-guidance/drug-offences>
14. Dams R, Benijts T, Lambert W. Heroin impurity profiling: trends throughout a decade of experimenting. *Forensic Sci* [Internet]. 2001 [cited 2014 Oct 21];123:81–8. Available from: <http://www.sciencedirect.com/science/article/pii/S0379073801005412>
15. Cole, D.D., (2003). Chapter 5 Diamorphine and Heroin. *The Analysis of Controlled Substances*. (John Wiley & Sons)
16. World Drug Report: Opium/heroin (2012) United Nations Office on Drugs and Crime (Online). Available from the United Nations Office on Drugs and Crime. [Accessed on 21/05/2022]
17. CALA MA, GALLEJA JMG, CAULKINS J, DEHNE J, REUTER P, SABIN K. World Drug Report 2014.
18. United Nations Office for Drug Control and Crime Prevention, *Drug Characterization/Impurity Profiling* (United Nations Publication Sales No. E.01.XI.10).
19. Home Office. Seizures of drugs in England. 2014;1–18.
20. Zerell U, Ahrens B, Gerz P. Documentation of a heroin manufacturing process in Afghanistan. *Bull Narc.* 2007;57(1–2):11–31.
21. Division of Narcotic Drugs, Recommended methods for testing heroin. Manual for Use by National Narcotics Laboratories, United Nations, New York, USA, 1986.
22. Paul, B.D. and Smith, M.L., LSD-An overview on drug action and detection, *forensic science rev.*, 11(1999) 157-175
23. O’Neil PJ, Gough T a. Illicitly imported heroin products: some physical and chemical features indicative of their origin. Part II. *J Forensic Sci* [Internet]. 1985 Jul;30(3):681–91. Available from: <http://www.ncbi.nlm.nih.gov/pubmed/4031803>
24. Rendle D. Use of X-rays in the United Kingdom Forensic Science Service. *Adv X-ray Anal* [Internet]. 2003 [cited 2014 Oct 21];46:17–24. Available from:

- <http://scholar.google.com/scholar?hl=en&btnG=Search&q=intitle:USE+OF+X-RAYS+IN+THE+UNITED+KINGDOM+FORENSIC+SCIENCE#0>
25. Dujourdy L, Barbati G, Taroni F, Guéniat O, Esseiva P, Anglada F, et al. Evaluation of links in heroin seizures. *Forensic Sci Int*. 2003;131(2–3):171–83.
 26. Sharma SP, Purkait BC, Lahiri SC. Qualitative and quantitative analysis of seized street drug samples and identification of source. *Forensic Sci Int* [Internet]. 2005 Sep 10 [cited 2014 Aug 19];152(2–3):235–40. Available from: <http://www.ncbi.nlm.nih.gov/pubmed/15978350>
 27. Bühringer G, Farrell M, Kraus L, Marsden J, Pfeiffer-Gerschel T, Piontek D, et al. Comparative Analysis of Research into Illicit Drugs in the European Union. 2009.1–418 p.
 28. Costa P, Sousa Lobo JM. Ref 78. Vol. 13, *Eur. J. Pharm. Sci*. 2001. p. 123.
 29. United Nations Office on Drugs and Crime, Guidelines on Representative Drug Sampling (United Nations Publication Sales No. E.09.XI.13).
 30. Reported for 2007 -2008* Seizures of illicit laboratories manufacture, [Internet]. [cited 2023 Mar 20]. Available from: <https://www.unodc.org/documents/data-and-analysis/WDR2010/AllLabSeizures.pdf>
 31. Speakman SA. Basics of X-Ray Powder Diffraction Required Training to Become an Independent User in the X-Ray SEF at the Center for Materials Science and Engineering at MIT. (617). Available from: <http://prism.mit.edu/xray>
 32. Primer XD, Procedures I, Minerals IC, Mineral C, Flow I. A Laboratory Manual for X-Ray Powder Diffraction. 2002;
 33. Esseiva P, Ioset S, Anglada F, Gasté L, Ribaux O, Margot P, et al. Forensic drug intelligence: an important tool in law enforcement. *Forensic Sci Int* [Internet]. 2007 Apr 11 [cited 2014 Nov 5];167(2–3):247–54. Available from: <http://www.sciencedirect.com/science/article/pii/S0379073806004300>
 34. Roadmap for Seized Drug Analysis [Internet]. [cited 2023 Mar 20]. Available from: <https://www.nist.gov/system/files/documents/2020/05/01/FY2020%20OSAC%20Seized%20Drug%20Roadmap.pdf>

35. Esseiva P, Dujourdy L, Anglada F, Taroni F, Margot P. A methodology for illicit heroin seizures comparison in a drug intelligence perspective using large databases. *Forensic Sci Int.* 2003;132(2):139–52.
36. F. Besacier and H. Chaudron-Thozet, “Chemical profiling of illicit heroin samples”, *Forensic Science Review*, vol. 11, No. 2 (1999), pp. 105-119.
37. Rendle DF. *Advances in chemistry applied to forensic science.* Chem Soc Rev [Internet]. 2005 Dec [cited 2014 Sep 4];34(12):1021–30. Available from: <http://www.ncbi.nlm.nih.gov/pubmed/16284668>
38. Morello DR, Cooper SD, Panicker S, Casale JF. Signature profiling and classification of illicit heroin by GC-MS analysis of acidic and neutral manufacturing impurities. *J Forensic Sci* [Internet]. 2010 Jan [cited 2014 Sep 5];55(1):42–9. Available from: <http://www.ncbi.nlm.nih.gov/pubmed/20002261>
39. Mihaela Gheorghe, Dan Bălălaşu Mihaela Ilie, Daniela-Luiza Baconi A-MC. Component Analysis of Illicit Heroin Samples By GC-MS Method. *Farmacia.* 2008;Vol.LVI(5).
40. Moffat, A.C., Osselton, M.D., (2011). *Clarkés Analysis of Drugs and Poisons.* Fourth edition. London: Pharmaceutical Press.
41. Mcnair, H.M., Miller, J.M. (2009). *Basic Gas Chromatography.* Second edition, New Jersey: John Wiley & Sons, Inc.
42. Ngim, K.K., Ebeler, S.E., Lew, M.E., Crosby, D.G. and Wong, J.W., (2000). Optimized
6. Procedures for Analyzing Primary Alkylamines in Wines by
Pentafluorobenzaldehyde
43. Derivatization and GC-MS. *Journal of Agricultural and Food Chemistry*, 48(8), pp. 3311-
7. 3316.
44. Skender, L., Karacic, V., Brcic, I., Bagaric, A., (2002), Quantitative determination of
8. amphetamines, cocaine and opiates in human hair by gas chromatograph/
mass
9. spectrometry. *Forensic Science International.* Elsevier. pp 120-126
45. DeWitt K, Richards-Waugh L, Professor A. X-Ray Powder Diffraction Method Development and Validation for the Identification of Counterfeit Pharmaceuticals. *Oh.* 2253;45237(513):679–2700.

46. The Gnu Xtal System User's Manual Prev Chapter 4. Reference Manual
https://www.iucr.org/__data/iucr/cif/software/xtal/xtal372htmlman/html/latcon-desc.html
47. Rasmussen, K.E. and Knutsen, P., Techniques for the Detection and Identification of Amphetamines and Amphetamine-like Substances, *Narc.*, Issue 1, (1985) 95-112
48. European Monitoring Centre for Drugs and Drug Addiction (2020), European Drug Report 2020: Trends and Developments, Publications Office of the European Union, Luxembourg
49. Madsen IC, Hill RJ. Effect of divergence and receiving slit dimensions on peak profile parameters in Rietveld analysis of X-ray diffractometer data. Vol. 21, *Journal of Applied Crystallography*. 1988. p. 398–405.
50. Jurásek B, Bartůněk V, Huber Š, Kuchař M. X-Ray powder diffraction – A non-destructive and versatile approach for the identification of new psychoactive substances. *Talanta* [Internet]. 2019;195(August 2018):414–8. Available from: <https://doi.org/10.1016/j.talanta.2018.11.063>
51. Roller J. X-ray diffraction. *PEM Fuel Cell Diagnostic Tools*. 2011;289–313.
52. Jurásek B, Bartůněk V, Huber Š, Fagan P, Setnička V, Králík F, et al. Can X-Ray Powder Diffraction Be a Suitable Forensic Method for Illicit Drug Identification? *Front Chem*. 2020 Jun 23;8.
53. Guinebretière, R. (2013). *X-Ray Diffraction by Polycrystalline Materials*. Wiley ISTE. Guinebretière, R., Boule, A., Masson, O. & Dauger, A. (2005). *Powder Diffraction*. 20, 294.
54. Mittemeijer, E. J. & Scardi, P. (2004). *Diffraction Analysis of the Microstructure of Materials*, Springer Series in Materials Science. Berlin, Heidelberg: Springer-Verlag.
55. B.E. Warren, *X-ray diffraction* (Dover Publications, Inc., New York) 2nd Ed. 1990.
56. Fernando NK et al. Structural and Electronic Effects of X-ray Irradiation on Prototypical [M (COD) Cl] 2 Catalysts. *The Journal of Physical Chemistry A* 125, 34, 7473–7488 (2021). DOI: 10.1021/acs.jpca.1c05759.

57. S'ari M, Cattle J, Hondow N, Blade H, Cosgrove S, Brydson RM, et al. Analysis of Electron Beam Damage of Crystalline Pharmaceutical Materials by Transmission Electron Microscopy. *Journal of Physics: Conference Series*. 2015 Oct 12;644:012038.
58. UCSB Physics, (2008). Amorphous materials. [Accessed from: <http://web.physics.ucsb.edu/~complex/research/amorphous.html>] [Accessed on 14/12/2013]
59. H. Neumann and M. Gloger, "Profiling of illicit heroin samples by highresolution capillary gas chromatography for forensic application", *Chromatographia*, vol. 16, 1982, pp. 261-264.
60. Zallen R., (2014). Amorphous solid, *Encyclopaedia Britannica*. [Accessed from: <http://www.britannica.com/EBchecked/topic/21328/amorphous-solid>] [Accessed on 14/12/2013]
61. Bates.S, Zografi.G, Engers. D, et al. (2006), Analysis of Amorphous and Nanocrystalline 10. Solids from Their X-Ray Diffraction Patterns. *Pharmaceutical Research*. 23(10), pp 2333-2349.
62. Esseiva P, Anglada F, Dujourdy L, Taroni F, Margot P, Pasquier E Du, et al. Chemical profiling and classification of illicit heroin by principal component analysis, calculation of inter sample correlation and artificial neural networks. *Talanta* [Internet]. 2005 Aug 15 [cited 2014 Sep 5];67(2):360–7. Available from: <http://www.ncbi.nlm.nih.gov/pubmed/18970176>
63. Morelato M, Beavis A, Tahtouh M, Ribaux O, Kirkbride P, Roux C. The use of forensic case data in intelligence-led policing: the example of drug profiling. *Forensic Sci Int* [Internet]. 2013 Mar 10 [cited 2014 Nov 1];226(1–3):1–9. Available from: <http://www.sciencedirect.com/science/article/pii/S0379073813000066>
64. Dégardin K, Roggo Y, Been F, Margot P. Detection and chemical profiling of medicine counterfeits by Raman spectroscopy and chemometrics. *Anal Chim Acta* [Internet]. 2011 Oct 31 [cited 2014 Nov 4];705(1–2):334–41. Available from: <http://www.sciencedirect.com/science/article/pii/S0003267011010439>
65. H. Huizer, "Analytical studies on illicit heroin: I. The occurrence of O3-monoacetylmorphine", *Journal of Forensic Sciences*, vol. 28, No. 1 (1983), pp. 32-39.

66. Chiarotti, M., Fucci, N. and Furnari, C., Comparative analysis of illicit heroin samples, *Forensic Sci. Int.*, 50 (1991) 47-55
67. N. Döbelin, "Lecture Handouts", Lesson 5: Rietveld Refinement, http://profex.doebelin.org/?page_id=68.20 H.M. Rietveld, *Acta Cryst.* 22, 151-2 (1967).
68. Dufey V, Dujourdy L, Besacier F, Chaudron H. A quick and automated method for profiling heroin samples for tactical intelligence purposes. *Forensic Sci ...* [Internet]. 2007 [cited 2014 Sep 4];169:108–17. Available from: <http://www.sciencedirect.com/science/article/pii/S0379073806005329>
69. Dams R, Benijts T, Lambert W. Heroin impurity profiling: trends throughout a decade of experimenting. *Forensic Sci* [Internet]. 2001 [cited 2014 Oct 21];123:81–8. Available from: <http://www.sciencedirect.com/science/article/pii/S0379073801005412>
70. Kugler W. X-ray diffraction analysis in the forensic science: the last resort in many criminal cases. *Adv X-ray Anal* [Internet]. 2003 [cited 2014 Oct 21];46:1–16. Available from: <http://spectrolab.co.uk/pages/txrf/pdf/XDR-forensic.pdf>
71. Connolly J. Introduction to X-ray Powder Diffraction. In 2007. p. 1–9.
72. Australian Crime Commission - Illicit Drug Data Report 2012–13.
73. R.A. Young (ed.), "The Rietveld Method", International Union of Crystallography, Oxford University Press, New York 1993.
74. Guinebretière, R. (2013). *X-Ray Diffraction by Polycrystalline Materials*. Wiley-ISTE. Guinebretière, R., Boule, A., Masson, O. & Dauger, A. (2005). *Powder Diffraction*. 20, 294
75. H.M. Rietveld, *J. Appl. Cryst.* 2, 65-71 (1969).
76. Mittemeijer, E. J. & Scardi, P. (2004). *Diffraction Analysis of the Microstructure of Materials*, Springer Series in Materials Science. Berlin, Heidelberg: Springer-Verlag.
77. Al Hassan A, Lähnemann J, Davtyan A, Al-Humaidi M, Herranz J, Bahrami D, et al. Beam damage of single semiconductor nanowires during X-ray nanobeam diffraction experiments. *Journal of Synchrotron Radiation*. 2020 Aug 12;27(5):1200–8.

78. Refine lattice parameters [Internet]. www.iucr.org. Available from: https://www.iucr.org/_data/iucr/cif/software/xtal/xtal372htmlman/html/latcon-desc.html
79. Bates.S, Zografi.G, Engers. D, et al. (2006), Analysis of Amorphous and Nanocrystalline Solids from Their X-Ray Diffraction Patterns. *Pharmaceutical Research*. 23(10), pp 2333-2349.
80. Glaeser.R. Characterization of Conditions Required for X-Ray Diffraction Experiments with Protein Microcrystals | Elsevier Enhanced Reader [Internet]. 2000; Available from: <https://reader.elsevier.com/reader/sd/pii/S0006349500768548?token=FC9B297DBF20523381E6E2733FC44D5F1CBE722094BD83BDE5672566DB8DA1601F1E18A59B682C3DBFD34DFBDB11C597>
81. Nave C. Radiation damage in protein crystallography. *Radiat Phys Chem*.1995;45(3):483–90.
82. Connolly J. Introduction quantitative X-ray diffraction methods. Note cours EPS400-002, Univ New Mex [Internet]. 2003 [cited 2014 Oct 21];1–15. Available from: <http://scholar.google.com/scholar?hl=en&btnG=Search&q=intitle:Introduction+Quantitative+X-Ray+Diffraction+Methods#0>
83. Connolly J. Systematic Errors and Sample Preparation for X-Ray Powder Diffraction.2010

Appendix 1- Extra data

Comments	Keys
The parameter is written in the following order: Angular Range (A), Step size, Steps, Step time	D- Diamorphine
	Co- Codeine
	P- Paracetamol
	Ca-Caffeine
	S- Sucrose
	BH- Bruker Holder (Transmission)
	PH-Proposed Holder (Transmission)
	T- Transmission
	R- Reflection
	V- Time
	A- Angular Range
	I- Increment
	Slit used- 0.2mm or 0.6mm
V1A2I2	10mins, 5-70°, 0.040

V1A3I3	10mins,5-80°, 0.060
V1A5I5	10mins, 5-100°, 0.10
V1A4I4	10mins, 5-90°, 0.080
V2A1I1	20mins, 5-60°,0.020
V2A3I3	20mins,5-70°, 0.060
V2A2I2	20mins, 5-70°, 0.040
VOA1I1	
V0.5A1I1	5mins, 5-60°, 0.020
V1A1I1	10mins, 5-60°, 0.020
V2A5I5	20mins, 5-100°, 0.10
V3A2I2	30mins, 5-70°, 0.040
V3A4I4	30mins, 5-90°, 0.080
V3A1I1	30mins, 5-60°,0.020

Sample name	Date of analysis	Reflection or Transmission	Holder used	Parameter
Blank_V3A1I1	28/09/2016	T	Bruker T holder	5-60°, 0.020°,

				2701, 122.88s
D50Co50_1_BH_V3A1I1_0.6mm	28/09/20 16	T	Bruker T holder	5-60°, 0.020°, 2701, 122.88s
D50Co50_2_BH_V3A1I1_0.6mm	28/09/20 16	T	Bruker T holder	5-60°, 0.020°, 2701, 122.88s
D50Co50_3_BH_V3A1I1_0.6mm	28/09/20 16	T	Bruker T holder	5-60°, 0.020°, 2701, 122.88s
P33.3Ca33.3S33.3_1_BH_V3A1I1_0.6mm	28/09/20 16	T	Bruker T holder	5-60°, 0.020°, 2701, 122.88s
P33.3Ca33.3S33.3_2_BH_V3A1I1_0.6mm	28/09/20 16	T	Bruker T holder	5-60°, 0.020°, 2701, 122.88s
P33.3Ca33.3S33.3_3_BH_V3A1I1_0.6mm	28/09/20 16	T	Bruker T holder	5-60°, 0.020°, 2701, 122.88s

P50Co50_1_BH_V3A1I1_0.6mm	28/09/20 16	T	Bruker T holder	5-60°, 0.020°, 2701, 122.88s
P50Co50_2_BH_V3A1I1_0.6mm	28/09/20 16	T	Bruker T holder	5-60°, 0.020°, 2701, 122.88s
P50Co50_3_BH_V3A1I1_0.6mm	28/09/20 16	T	Bruker T holder	5-60°, 0.020°, 2701, 122.88s
P50Ca50_1_BH_V3A1I1_0.6mm	28/09/20 16	T	Bruker T holder	5-60°, 0.020°, 2701, 122.88s
P50Ca50_2_BH_V3A1I1_0.6mm	28/09/20 16	T	Bruker T holder	5-60°, 0.020°, 2701, 122.88s
P50Ca50_3_BH_V3A1I1_0.6mm	28/09/20 16	T	Bruker T holder	5-60°, 0.020°, 2701, 122.88s
Blank_V2A4I4_0.6mm	02/09/20 16	T	Bruker T holder	5-90°, 0.080°

				1058, 211.20s
D50Co50_1_BH_V2A4I4_0.6mm	02/09/20 16	T	Bruker T holder	5-90°, 0.080°, 1058, 211.20s
D50Co50_2_BH_V2A4I4_0.6mm	02/09/20 16	T	Bruker T holder	5-90°, 0.080°, 1058, 211.20s
D50Co50_3_BH_V2A4I4_0.6mm	02/09/20 16	T	Bruker T holder	5-90°, 0.080°, 1058, 211.20s
P33.3Ca33.3S33.3_1_BH_V2A4I4_0.6mm	02/09/20 16	T	Bruker T holder	5-90°, 0.080°, 1058, 211.20s
P33.3Ca33.3S33.3_2_BH_V2A4I4_0.6mm	02/09/20 16	T	Bruker T holder	5-90°, 0.080°, 1058, 211.20s
P33.3Ca33.3S33.3_3_BH_V2A4I4_0.6mm	02/09/20 16	T	Bruker T holder	5-90°, 0.080°, 1058, 211.20s

P50Co50_1_BH_V2A4I4_0.6mm	02/09/20 16	T	Bruker T holder	5-90°, 0.080°, 1058, 211.20s
P50Co50_2_BH_V2A4I4_0.6mm	02/09/20 16	T	Bruker T holder	5-90°, 0.080°, 1058, 211.20s
P50Co50_3_BH_V2A4I4_0.6mm	02/09/20 16	T	Bruker T holder	5-90°, 0.080°, 1058, 211.20s
P50Ca50_1_BH_V2A4I4_0.6mm	02/09/20 16	T	Bruker T holder	5-90°, 0.080°, 1058, 211.20s
P50Ca50_2_BH_V2A4I4_0.6mm	02/09/20 16	T	Bruker T holder	5-90°, 0.080°, 1058, 211.20s
P50Ca50_3_BH_V2A4I4_0.6mm	02/09/20 16	T	Bruker T holder	5-90°, 0.080°, 1058, 211.20s
P50Ca50_3_BH_V2A1I1	14/08/20 16	T	Bruker T holder	5-60°, 0.020°

				2703, 24.00s
P50Ca50_1_PH_V2A1I1	14/08/20 16	T	Proposed Holder	5-60°, 0.020°, 2703, 24.00s
P50Ca50_2_PH_V2A1I1	14/08/20 16	T	Proposed Holder	5-60°, 0.020°, 2703, 24.00s
P50Ca50_3_PH_V2A1I1	14/08/20 16	T	Proposed Holder	5-60°, 0.020°, 2703, 24.00s
F0356_11_1.2_1_130416_V1A1I 1	13/04/20 16	T	Bruker T holder	5-60°, 0.020°, 2703, 42.24s
F0356_11_1.2_2_130416_V1A1I 1	13/04/20 16	T	Bruker T holder	5-60°, 0.020°, 2703, 42.24s
F0356_11_1.2_3_130416_V1A1I 1	13/04/20 16	T	Bruker T holder	5-60°, 0.020°, 2703, 42.24s

F6723.10_1.3_1_130416_V1A11 1	13/04/20 16	T	Bruker T holder	5-60°, 0.020°, 2703, 42.24s
F6723.10_1.3_2_130416_V1A11 1	13/04/20 16	T	Bruker T holder	5-60°, 0.020°, 2703, 42.24s
F6723.10_1.3_3_130416_V1A11 1	13/04/20 16	T	Bruker T holder	5-60°, 0.020°, 2703, 42.24s
JCD1_1_130416_V1A111	13/04/20 16	T	Bruker T holder	5-60°, 0.020°, 2703, 42.24s
JCD1_2_130416_V1A111	13/04/20 16	T	Bruker T holder	5-60°, 0.020°, 2703, 42.24s
JCD1_3_130416_V1A111	13/04/20 16	T	Bruker T holder	5-60°, 0.020°, 2703, 42.24s
P50Co50_1_130416_V1A111	13/04/20 16	T	Bruker T holder	5-60°, 0.020°

				2703, 42.24s
P50Co50_2_130416_V1A1I1	13/04/20 16	T	Bruker T holder	5-60°, 0.020°, 2703, 42.24s
P50Co50_3_130416_V1A1I1	13/04/20 16	T	Bruker T holder	5-60°, 0.020°, 2703, 42.24s
F0356_11_1.2_1_130416_V0.5A 1I1	13/04/20 16	T	Bruker T holder	5-60°, 0.020°, 2703, 32.64s
F0356_11_1.2_2_130416_V0.5A 1I1	13/04/20 16	T	Bruker T holder	5-60°, 0.020°, 2703, 32.64s
F0356_11_1.2_3_130416_V0.5A 1I1	13/04/20 16	T	Bruker T holder	5-60°, 0.020°, 2703, 32.64s
F6723.10_1.3_1_130416_V0.5A 1I1	13/04/20 16	T	Bruker T holder	5-60°, 0.020°, 2703, 32.64s

F6723.10_1.3_2_130416_V0.5A1I1	13/04/20 16	T	Bruker T holder	5-60°, 0.020°, 2703, 32.64s
F6723.10_1.3_3_130416_V0.5A1I1	13/04/20 16	T	Bruker T holder	5-60°, 0.020°, 2703, 32.64s
JCD1_1_130416_V0.5A1I1	13/04/20 16	T	Bruker T holder	5-60°, 0.020°, 2703, 32.64s
JCD1_2_130416_V0.5A1I2	13/04/20 16	T	Bruker T holder	5-60°, 0.020°, 2703, 32.64s
JCD1_3_130416_V0.5A1I3	13/04/20 16	T	Bruker T holder	5-60°, 0.020°, 2703, 32.64s
P50Co50_1_130416_V0.5A1I1	13/04/20 16	T	Bruker T holder	5-60°, 0.020°, 2703, 32.64s
P50Co50_2_130416_V0.5A1I1	13/04/20 16	T	Bruker T holder	5-60°, 0.020°,

				2703, 32.64s
P50Co50_3_130416_V0.5A1I1	13/04/20 16	T	Bruker T holder	5-60°, 0.020°, 2703, 32.64s
F0356_11_1.2_1_V2A1I1_06041 6	06/04/20 16	T	Bruker T holder	5-60°, 0.020°, 2701, 82.56s
F0356_11_1.2_2_V2A1I1_06041 6	06/04/20 16	T	Bruker T holder	5-60°, 0.020°, 2701, 82.56s
F0356_11_1.2_3_V2A1I1_06041 6	06/04/20 16	T	Bruker T holder	5-60°, 0.020°, 2701, 82.56s
F6723.10_1.3_1_V2A1I1_06041 6	06/04/20 16	T	Bruker T holder	5-60°, 0.020°, 2701, 82.56s
F6723.10_1.3_2_V2A1I1_06041 6	06/04/20 16	T	Bruker T holder	5-60°, 0.020°, 2701, 82.56s

F6723.10_1.3_3_V2A1I1_060416	06/04/2016	T	Bruker T holder	5-60°, 0.020°, 2701, 82.56s
JCD1_1_V2A1I1_060416	06/04/2016	T	Bruker T holder	5-60°, 0.020°, 2701, 82.56s
JCD1_2_V2A1I2_060416	06/04/2016	T	Bruker T holder	5-60°, 0.020°, 2701, 82.56s
JCD1_3_V2A1I3_060416	06/04/2016	T	Bruker T holder	5-60°, 0.020°, 2701, 82.56s
P50Co50_1_V2A1I1_060416	06/04/2016	T	Bruker T holder	5-60°, 0.020°, 2701, 82.56s
P50Co50_2_V2A1I1_060416	06/04/2016	T	Bruker T holder	5-60°, 0.020°, 2701, 82.56s
P50Co50_3_V2A1I1_060416	06/04/2016	T	Bruker T holder	5-60°, 0.020°,

				2701, 82.56s
P50Ca50_1_BH_V6A2I2	30/09/20 15	T	Bruker T holder	5-60°, 0.020°, 2704, 243.84s
P50Ca50_2_BH_V6A2I2	30/09/20 15	T	Bruker T holder	5-60°, 0.020°, 2704, 243.84s
P50Ca50_3_BH_V6A2I2	30/09/20 15	T	Bruker T holder	5-60°, 0.020°, 2704, 243.84s
P50Co50_1_BH_V6A2I2	30/09/20 15	T	Bruker T holder	5-60°, 0.020°, 2704, 243.84s
P50Co50_2_BH_V6A2I2	30/09/20 15	T	Bruker T holder	5-60°, 0.020°, 2704, 243.84s
P50Co50_3_BH_V6A2I2	30/09/20 15	T	Bruker T holder	5-60°, 0.020°, 2704, 243.84s

D50Co50_1_BH_V3A2I2_0.6mm	29/09/20 15	T	Bruker T holder	5-70°, 0.040°, 1638, 203.52s
D50Co50_2_BH_V3A.2I2_0.6mm	29/09/20 15	T	Bruker T holder	5-70°, 0.040°, 1638, 203.52s
D50Co50_3_BH_V3A2I2_0.6mm	29/09/20 15	T	Bruker T holder	5-70°, 0.040°, 1638, 203.52s
P33.3Ca33.3S33.3_1_BH_V3A2I2_0.6mm	29/09/20 15	T	Bruker T holder	5-70°, 0.040°, 1638, 203.52s
P33.3Ca33.3S33.3_2_BH_V3A2I2_0.6mm	29/09/20 15	T	Bruker T holder	5-70°, 0.040°, 1638, 203.52s
P33.3Ca33.3S33.3_3_BH_V3A2I2_0.6mm	29/09/20 15	T	Bruker T holder	5-70°, 0.040°, 1638, 203.52s
P50Co50_1_BH_V3A2I2_0.6mm	29/09/20 15	T	Bruker T holder	5-70°, 0.040°

				1638, 203.52s
P50Co50_2_BH_V3A2I2_0.6mm	29/09/20 15	T	Bruker T holder	5-70°, 0.040°, 1638, 203.52s
P50Co50_3_BH_V3A2I2_0.6mm	29/09/20 15	T	Bruker T holder	5-70°, 0.040°, 1638, 203.52s
P50Ca50_1_BH_V3A2I2_0.6mm	29/09/20 15	T	Bruker T holder	5-70°, 0.040°, 1638, 203.52s
P50Ca50_2_BH_V3A2I2_0.6mm	29/09/20 15	T	Bruker T holder	5-70°, 0.040°, 1638, 203.52s
P50Ca50_3_BH_V3A2I2_0.6mm	29/09/20 15	T	Bruker T holder	5-70°, 0.040°, 1638, 203.52s
Blank_V2A5I5_0.6mm	04/09/20 15	T	Bruker T holder	5-90°, 0.100°, 853, 261.12s

D50Co50_1_BH_V2A5I5_0.6mm	04/09/20 15	T	Bruker T holder	5-90°, 0.100°, 853, 261.12s
D50Co50_2_BH_V2A5I5_0.6mm	04/09/20 15	T	Bruker T holder	5-90°, 0.100°, 853, 261.12s
D50Co50_3_BH_V2A5I5_0.6mm	04/09/20 15	T	Bruker T holder	5-90°, 0.100°, 853, 261.12s
P33.3Ca33.3S33.3_1_BH_V2A5I5_0.6mm	04/09/20 15	T	Bruker T holder	5-90°, 0.100°, 853, 261.12s
P33.3Ca33.3S33.3_2_BH_V2A5I5_0.6mm	04/09/20 15	T	Bruker T holder	5-90°, 0.100°, 853, 261.12s
P33.3Ca33.3S33.3_3_BH_V2A5I5_0.6mm	04/09/20 15	T	Bruker T holder	5-90°, 0.100°, 853, 261.12s
P50Co50_1_BH_V2A5I5_0.6mm	04/09/20 15	T	Bruker T holder	5-90°, 0.100°,

				853, 261.12s
P50Co50_2_BH_V2A5I5_0.6mm	04/09/20 15	T	Bruker T holder	5-90°, 0.100°, 853, 261.12s
P50Co50_3_BH_V2A5I5_0.6mm	04/09/20 15	T	Bruker T holder	5-90°, 0.100°, 853, 261.12s
P50Ca50_1_BH_V2A5I5_0.6mm	04/09/20 15	T	Bruker T holder	5-90°, 0.100°, 853, 261.12s
P50Ca50_2_BH_V2A5I5_0.6mm	04/09/20 15	T	Bruker T holder	5-90°, 0.100°, 853, 261.12s
P50Ca50_3_BH_V2A5I5_0.6mm	04/09/20 15	T	Bruker T holder	5-90°, 0.100°, 853, 261.12s
Blank_V1A1I1_0.2	02/09/20 15	T	Bruker T holder	5-60°, 0.020°, 2703, 42.24s

D50Co50_1_BH_V1A1I1_0.2mm	02/09/20 15	T	Bruker T holder	5-60°, 0.020°, 2703, 42.24s
D50Co50_2_BH_V1A1I1_0.2mm	02/09/20 15	T	Bruker T holder	5-60°, 0.020°, 2703, 42.24s
D50Co50_3_BH_V1A1I1_0.2mm	02/09/20 15	T	Bruker T holder	5-60°, 0.020°, 2703, 42.24s
P33.3Ca33.3S33.3_1_BH_V1A1I1_0.2mm	02/09/20 15	T	Bruker T holder	5-60°, 0.020°, 2703, 42.24s
P33.3Ca33.3S33.3_2_BH_V1A1I1_0.2mm	02/09/20 15	T	Bruker T holder	5-60°, 0.020°, 2703, 42.24s
P33.3Ca33.3S33.3_3_BH_V1A1I1_0.2mm	02/09/20 15	T	Bruker T holder	5-60°, 0.020°, 2703, 42.24s
P50Co50_1_BH_V1A1I1_0.2mm	02/09/20 15	T	Bruker T holder	5-60°, 0.020°,

				2703, 42.24s
P50Co50_2_BH_V1A1I1_0.2mm	02/09/20 15	T	Bruker T holder	5-60°, 0.020°, 2703, 42.24s
P50Co50_3_BH_V1A1I1_0.2mm	02/09/20 15	T	Bruker T holder	5-60°, 0.020°, 2703, 42.24s
Blank_V1A2I2_T1_0.2mm	02/09/20 15	T	Bruker T holder	5-70°, 0.040°, 1638, 69.12s
D50Co50_1_BH_V1A2I2_0.2mm	02/09/20 15	T	Bruker T holder	5-70°, 0.040°, 1638, 69.12s
D50Co50_2_BH_V1A2I2_0.2mm	02/09/20 15	T	Bruker T holder	5-70°, 0.040°, 1638, 69.12s
D50Co50_3_BH_V1A2I2_0.2mm	02/09/20 15	T	Bruker T holder	5-70°, 0.040°, 1638, 69.12s

P33.3Ca33.3S33.3_1_BH_V1A2I2_0.2mm	02/09/20 15	T	Bruker T holder	5-70°, 0.040°, 1638, 69.12s
P33.3Ca33.3S33.3_2_BH_V1A2I2_0.2mm	02/09/20 15	T	Bruker T holder	5-70°, 0.040°, 1638, 69.12s
P33.3Ca33.3S33.3_3_BH_V1A2I2_0.2mm	02/09/20 15	T	Bruker T holder	5-70°, 0.040°, 1638, 69.12s
P50Co50_1_BH_V1A2I2_0.2mm	02/09/20 15	T	Bruker T holder	5-70°, 0.040°, 1638, 69.12s
P50Co50_2_BH_V1A2I2_0.2mm	02/09/20 15	T	Bruker T holder	5-70°, 0.040°, 1638, 69.12s
P50Co50_3_BH_V1A2I2_0.2mm	02/09/20 15	T	Bruker T holder	5-70°, 0.040°, 1638, 69.12s
P50Ca50_1_BH_V1A2I2_0.2mm	02/09/20 15	T	Bruker T holder	5-70°, 0.040°,

				1638, 69.12s
P50Ca50_2_BH_V1A2I2_0.2mm	02/09/20 15	T	Bruker T holder	5-70°, 0.040°, 1638, 69.12s
P50Ca50_3_BH_V1A2I2_0.2mm	02/09/20 15	T	Bruker T holder	5-70°, 0.040°, 1638, 69.12s
Blank_010915	01/09/20 15	T	Bruker T holder	5-60°, 0.020°, 2703, 42.24s
D50Co50_1_BH_V1A1I1_0.6mm	01/09/20 15	T	Bruker T holder	5-60°, 0.020°, 2703, 42.24s
D50Co50_2_BH_V1A1I1_0.6mm	01/09/20 15	T	Bruker T holder	5-60°, 0.020°, 2703, 42.24s
D50Co50_3_BH_V1A1I1_0.6mm	01/09/20 15	T	Bruker T holder	5-60°, 0.020°, 2703, 42.24s

P33.3Ca33.3S33.3_1_BH_V1A1I1_0.6mm	01/09/20 15	T	Bruker T holder	5-60°, 0.020°, 2703, 42.24s
P33.3Ca33.3S33.3_2_BH_V1A1I1_0.6mm	01/09/20 15	T	Bruker T holder	5-60°, 0.020°, 2703, 42.24s
P33.3Ca33.3S33.3_3_BH_V1A1I1_0.6mm	01/09/20 15	T	Bruker T holder	5-60°, 0.020°, 2703, 42.24s
P50Co50_1_BH_V1A1I1_0.6mm	01/09/20 15	T	Bruker T holder	5-60°, 0.020°, 2703, 42.24s
P50Co50_2_BH_V1A1I1_0.6mm	01/09/20 15	T	Bruker T holder	5-60°, 0.020°, 2703, 42.24s
P50Co50_3_BH_V1A1I1_0.6mm	01/09/20 15	T	Bruker T holder	5-60°, 0.020°, 2703, 42.24s
P50Ca50_1_BH_Longrun_0.6	01/09/20 15	T	Bruker T holder	10-60°, 0.002°,

				20251, 48.00s
P50Ca50_1_PH_Longrun_0.6	01/09/20 15	T	Proposed Holder	10-60°, 0.002°, 20251, 48.00s
P50Ca50_1_BH_V1A1I1_0.2mm	28/08/20 15	T	Bruker T holder	5-60°, 0.020°, 2703, 42.24s
P50Ca50_2_BH_V1A1I1_0.2mm	28/08/20 15	T	Bruker T holder	5-60°, 0.020°, 2703, 42.24s
P50Ca50_3_BH_V1A1I1_0.2mm	28/08/20 15	T	Bruker T holder	5-60°, 0.020°, 2703, 42.24s
P50Ca50_1_PH_V1A1I1_0.2mm	28/08/20 15	T	Proposed Holder	5-60°, 0.020°, 2703, 42.24s
P50Ca50_2_PH_V1A1I1_0.2mm	28/08/20 15	T	Proposed Holder	5-60°, 0.020°, 2703, 42.24s

P50Ca50_3_PH_V1A1I1_0.2mm	28/08/20 15	T	Proposed Holder	5-60°, 0.020°, 2703, 42.24s
Blank_V0.5A1I1	28/08/20 15	T	Bruker T holder	5-60°, 0.020°, 2703, 32.64s
P50Ca50_1_BH_V0.5A1I1_0.2m m	28/08/20 15	T	Bruker T holder	5-60°, 0.020°, 2703, 32.64s
P50Ca50_2_BH_V0.5A1I1_0.2m m	28/08/20 15	T	Bruker T holder	5-60°, 0.020°, 2703, 32.64s
P50Ca50_3_BH_V0.5A1I1_0.2m m	28/08/20 15	T	Bruker T holder	5-60°, 0.020°, 2703, 32.64s
P50Ca50_1_PH_V0.5A1I1_0.2m m	28/08/20 15	T	Proposed Holder	5-60°, 0.020°, 2703, 32.64s
P50Ca50_2_PH_V0.5A1I1_0.2m m	28/08/20 15	T	Proposed Holder	5-60°, 0.020°,

				2703, 32.64s
P50Ca50_3_PH_V0.5A1I1_0.2m m	28/08/20 15	T	Proposed Holder	5-60°, 0.020°, 2703, 32.64s
P50Ca50_BH_Longrun_0.2mm	28/08/20 15	T	Bruker T holder	10-60°, 0.0020°, 20251, 42.24s
P50Ca50_PH_Longrun_0.2mm	28/08/20 15	T	Proposed Holder	10-60°, 0.0020°, 20251, 42.24s
Blank_1_BH_V0A1I1	28/08/20 15	T	Bruker T holder	5-60°, 0.020°, 2703, 24.00s
P50Ca50_1_BH_V0A1I1	28/08/20 15	T	Bruker T holder	5-60°, 0.020°, 2703, 24.00s
P50Ca50_2_BH_V0A1I1	28/08/20 15	T	Bruker T holder	5-60°, 0.020°, 2703, 24.00s

P50Ca50_3_BH_V0A1I1	28/08/20 15	T	Bruker T holder	5-60°, 0.020°, 2703, 24.00s
P50Ca50_1_PH_V0A1I1	28/08/20 15	T	Proposed Holder	5-60°, 0.020°, 2703, 24.00s
P50Ca50_2_PH_V0A1I1	28/08/20 15	T	Proposed Holder	5-60°, 0.020°, 2703, 24.00s
P50Ca50_3_PH_V0A1I1	28/08/20 15	T	Proposed Holder	5-60°, 0.020°, 2703, 24.00s
Blank_BH_V2A2I2	26/08/20 15	T	Bruker T holder	5-70°, 0.040°, 1639, 136.32s
P50Ca50_1_BH_V2A2I2	26/08/20 15	T	Bruker T holder	5-70°, 0.040°, 1639, 136.32s
P50Ca50_2_BH_V2A2I2	26/08/20 15	T	Bruker T holder	5-70°, 0.040°,

				1639, 136.32s
P50Ca50_3_BH_V2A2I2	26/08/20 15	T	Bruker T holder	5-70°, 0.040°, 1639, 136.32s
P50Ca50_1_PH_V2A2I2	26/08/20 15	T	Proposed Holder	5-70°, 0.040°, 1639, 136.32s
P50Ca50_2_PH_V2A2I2	26/08/20 15	T	Proposed Holder	5-70°, 0.040°, 1639, 136.32s
P50Ca50_3_PH_V2A2I2	26/08/20 15	T	Proposed Holder	5-70°, 0.040°, 1639, 136.32s
Blank_BH_V2A3I3	26/08/20 15	T	Bruker T holder	5-80°, 0.060°, 1250, 178.56s
P50Ca50_1_BH_V2A3I3	26/08/20 15	T	Bruker T holder	5-80°, 0.060°, 1250, 178.56s

P50Ca50_2_BH_V2A3I3	26/08/20 15	T	Bruker T holder	5-80°, 0.060°, 1250, 178.56s
P50Ca50_3_BH_V2A3I3	26/08/20 15	T	Bruker T holder	5-80°, 0.060°, 1250, 178.56s
P50Ca50_1_PH_V2A3I3	26/08/20 15	T	Proposed Holder	5-80°, 0.060°, 1250, 178.56s
P50Ca50_2_PH_V2A3I3	26/08/20 15	T	Proposed Holder	5-80°, 0.060°, 1250, 178.56s
P50Ca50_3_PH_V2A3I3	26/08/20 15	T	Proposed Holder	5-80°, 0.060°, 1250, 178.56s
P50Ca50_1_BH_V2A1I1	14/08/20 15	T	Bruker T holder	5-60°, 0.020°, 2703, 24.00s
P50Ca50_2_BH_V2A1I1	14/08/20 15	T	Bruker T holder	5-60°, 0.020°,

				2703, 24.00s
Blank_BH_V1A4I4	14/08/20 15	T	Bruker T holder	5-90°, 0.080°, 1058, 105.60s
P50Ca50_1_BH_V1A4I4	14/08/20 15	T	Bruker T holder	5-90°, 0.080°, 1058, 105.60s
P50Ca50_2_BH_V1A4I4	14/08/20 15	T	Bruker T holder	5-90°, 0.080°, 1058, 105.60s
P50Ca50_3_BH_V1A4I4	14/08/20 15	T	Bruker T holder	5-90°, 0.080°, 1058, 105.60s
P50Ca50_1_PH_V1A4I4	14/08/20 15	T	Proposed Holder	5-90°, 0.080°, 1058, 105.60s
P50Ca50_2_PH_V1A4I4	14/08/20 15	T	Proposed Holder	5-90°, 0.080°, 1058, 105.60s

P50Ca50_3_PH_V1A4I4	14/08/20 15	T	Proposed Holder	5-90°, 0.080°, 1058, 105.60s
Blank_BH_V1A5I5	14/08/20 15	T	Bruker T holder	5-100°, 0.100°, 953, 119.04s
P50Ca50_1_BH_V1A5I5	14/08/20 15	T	Bruker T holder	5-100°, 0.100°, 953, 119.04s
P50Ca50_2_BH_V1A5I5	14/08/20 15	T	Bruker T holder	5-100°, 0.100°, 953, 119.04s
P50Ca50_3_BH_V1A5I5	14/08/20 15	T	Bruker T holder	5-100°, 0.100°, 953, 119.04s
P50Ca50_1_PH_V1A5I5	14/08/20 15	T	Proposed Holder	5-100°, 0.100°, 953, 119.04s
P50Ca50_2_PH_V1A5I5	14/08/20 15	T	Proposed Holder	5-100°, 0.100°,

				953, 119.04s
P50Ca50_3_PH_V1A5I5	14/08/20 15	T	Proposed Holder	5-100°, 0.100°, 953, 119.04s
Blank_BH_V1A3I3	13/08/20 15	T	Bruker T holder	5-80°, 0.060°, 1250, 90.24s
P50Ca50_1_BH_V1A3I3	13/08/20 15	T	Bruker T holder	5-80°, 0.060°, 1250, 90.24s
P50Ca50_2_BH_V1A3I3	13/08/20 15	T	Bruker T holder	5-80°, 0.060°, 1250, 90.24s
P50Ca50_3_BH_V1A3I3	13/08/20 15	T	Bruker T holder	5-80°, 0.060°, 1250, 90.24s
P50Ca50_1_PH_V1A3I3	13/08/20 15	T	Proposed Holder	5-80°, 0.060°, 1250, 90.24s

P50Ca50_2_PH_V1A3I3	13/08/20 15	T	Proposed Holder	5-80°, 0.060°, 1250, 90.24s
P50Ca50_3_PH_V1A3I3	13/08/20 15	T	Proposed Holder	5-80°, 0.060°, 1250, 90.24s
Blank_BH_V1A2I2	13/08/20 15	T	Bruker T holder	5-70°, 0.040°, 1638, 69.12s
P50Ca50_1_BH_V1A2I2	13/08/20 15	T	Bruker T holder	5-70°, 0.040°, 1638, 69.12s
P50Ca50_2_BH_V1A2I2	13/08/20 15	T	Bruker T holder	5-70°, 0.040°, 1638, 69.12s
P50Ca50_3_BH_V1A2I2	13/08/20 15	T	Bruker T holder	5-70°, 0.040°, 1638, 69.12s
P50Ca50_1_PH_V1A2I2	13/08/20 15	T	Proposed Holder	5-70°, 0.040°,

				1638, 69.12s
P50Ca50_2_PH_V1A2I2	13/08/20 15	T	Proposed Holder	5-70°, 0.040°, 1638, 69.12s
P50Ca50_3_PH_V1A2I2	13/08/20 15	T	Proposed Holder	5-70°, 0.040°, 1638, 69.12s
Codeine_100_R1_shortrun	13/08/20 15	R		5-70°, 0.020°, 1720, 96.00s
Codeine_100_R2_shortrun	13/08/20 15	R		5-70°, 0.020°, 1720, 96.00s
Codeine_100_R3_shortrun	13/08/20 15	R		5-70°, 0.020°, 1720, 96.00s
Codeine_100_R4_shortrun	13/08/20 15	R		5-70°, 0.020°, 1720, 96.00s

Codeine_100_R5_shortrun	13/08/20 15	R		5-70°, 0.020°, 1720, 96.00s
Caffeine_100_R1_shortrun	12/08/20 15	R		5-70°, 0.020°, 1720, 96.00s
Caffeine_100_R2_shortrun	12/08/20 15	R		5-70°, 0.020°, 1720, 96.00s
Caffeine_100_R3_shortrun	12/08/20 15	R		5-70°, 0.020°, 1720, 96.00s
Caffeine_100_R4_shortrun	12/08/20 15	R		5-70°, 0.020°, 1720, 96.00s
Caffeine_100_R5_shortrun	12/08/20 15	R		5-70°, 0.020°, 1720, 96.00s
Diamorphine_100_R1_shortrun	12/08/20 15	R		5-70°, 0.020°,

				1720, 96.00s
Diamorphine_100_R2_shortrun	12/08/20 15	R		5-70°, 0.020°, 1720, 96.00s
Diamorphine_100_R3_shortrun	12/08/20 15	R		5-70°, 0.020°, 1720, 96.00s
Diamorphine_100_R4_shortrun	12/08/20 15	R		5-70°, 0.020°, 1720, 96.00s
Diamorphine_100_R5_shortrun	12/08/20 15	R		5-70°, 0.020°, 1720, 96.00s
Paracetamol_100_R1_shortrun	12/08/20 15	R		5-70°, 0.020°, 1720, 96.00s
Paracetamol_100_R2_shortrun	12/08/20 15	R		5-70°, 0.020°, 1720, 96.00s

Paracetamol_100_R3_shortrun	12/08/20 15	R		5-70°, 0.020°, 1720, 96.00s
Paracetamol_100_R4_shortrun	12/08/20 15	R		5-70°, 0.020°, 1720, 96.00s
Paracetamol_100_R5_shortrun	12/08/20 15	R		5-70°, 0.020°, 1720, 96.00s
BD_Paracetamol_T1_BH_0.6mm	11/08/20 15	T	Bruker T holder	5-40°, 0.020°, 1720, 96.00s
BD_Paracetamol_T2_BH_0.6mm	11/08/20 15	T	Bruker T holder	5-40°, 0.020°, 1720, 96.00s
BD_Paracetamol_T3_BH_0.6mm	11/08/20 15	T	Bruker T holder	5-40°, 0.020°, 1720, 96.00s
BD_Paracetamol_T4_BH_0.6mm	11/08/20 15	T	Bruker T holder	5-40°, 0.020°,

				1720, 96.00s
BD_Paracetamol_T5_BH_0.6mm	11/08/20 15	T	Bruker T holder	5-40°, 0.020°, 1720, 96.00s
BD_Paracetamol_T1_PH_0.6mm	11/08/20 15	T	Proposed Holder	5-40°, 0.020°, 1720, 96.00s
BD_Paracetamol_T2_PH_0.6mm	11/08/20 15	T	Proposed Holder	5-40°, 0.020°, 1720, 96.00s
BD_Paracetamol_T3_PH_0.6mm	11/08/20 15	T	Proposed Holder	5-40°, 0.020°, 1720, 96.00s
BD_Paracetamol_T4_PH_0.6mm	11/08/20 15	T	Proposed Holder	5-40°, 0.020°, 1720, 96.00s
BD_Paracetamol_T5_PH_0.6mm	11/08/20 15	T	Proposed Holder	5-40°, 0.020°, 1720, 96.00s

T1_040615_no slit	04/06/20 15	T	Proposed Holder	5-60°, 0.020°, 2702, 96.00s
T2_040615_0.2mm	04/06/20 15	T	Proposed Holder	5-60°, 0.020°, 2702, 96.00s
T3_040615_0.6mm_BH	04/06/20 15	T	Bruker T holder	5-60°, 0.020°, 2702, 96.00s
T4_040615_0.2mm_BH	04/06/20 15	T	Bruker T holder	5-60°, 0.020°, 2702, 96.00s
BD_Paracetamol_T1_BH_0.2mm	10/05/20 15	T	Bruker T holder	5-40°, 0.020°, 1720, 96.00s
BD_Paracetamol_T2_BH_0.2mm	10/05/20 15	T	Bruker T holder	5-40°, 0.020°, 1720, 96.00s
BD_Paracetamol_T3_BH_0.2mm	10/05/20 15	T	Bruker T holder	5-40°, 0.020°,

				1720, 96.00s
BD_Paracetamol_T4_BH_0.2mm	10/05/20 15	T	Bruker T holder	5-40°, 0.020°, 1720, 96.00s
BD_Paracetamol_T5_BH_0.2mm	10/05/20 15	T	Bruker T holder	5-40°, 0.020°, 1720, 96.00s
BD_Paracetamol_T1_PH_0.2mm	10/05/20 15	T	Proposed Holder	5-40°, 0.020°, 1720, 96.00s
BD_Paracetamol_T2_PH_0.2mm	10/05/20 15	T	Proposed Holder	5-40°, 0.020°, 1720, 96.00s
BD_Paracetamol_T3_PH_0.2mm	10/05/20 15	T	Proposed Holder	5-40°, 0.020°, 1720, 96.00s
BD_Paracetamol_T4_PH_0.2mm	10/05/20 15	T	Proposed Holder	5-40°, 0.020°, 1720, 96.00s

BD_Paracetamol_T5_PH_0.2mm	10/05/20 15	T	Proposed Holder	5-40°, 0.020°, 1720, 96.00s
Holder_blank_Kapton_121214	12/12/20 14	T	Bruker T holder	5-60°, 0.020°, 2704, 96.00s
TM_Bruker_blank_Kapton_1212 14	12/12/20 14	T	Bruker T holder	5-60°, 0.020°, 2704, 96.00s
Lead(ii)Chloride_291014_longru n_32401	29/10/20 14	R	50mm diameter bruker standard	10-80°, 0.002°, 32401, 47.75s
P20Pb80_291014_longrun_3240 1	29/10/20 14	R	50mm diameter bruker standard	10-80°, 0.002°, 32401, 47.75s
P80Pb20_291014_longrun_3240 1	29/10/20 14	R	50mm diameter bruker standard	10-80°, 0.002°, 32401, 47.75s
Paracetamol_291014_longrun_3 2401	29/10/20 14	R	50mm diameter bruker standard	10-80°, 0.002°,

				32401, 47.75s
S50P50_291014_longrun_32401	29/10/20 14	R	50mm diameter bruker standard	10-80°, 0.002°, 32401, 47.75s
Sucrose_201014_longrun_32401	29/10/20 14	R	50mm diameter bruker standard	10-80°, 0.002°, 32401, 47.75s
Pb(NO ₂) ₃ _longrun_28001	29/10/20 14	R	50mm diameter bruker standard	0-70°, 0.002°, 28001, 47.75s
Lead(ii)chloride_291014_longrun_28001	29/10/20 14	R	50mm diameter bruker standard	0-70°, 0.002°, 28001, 47.75s
P20Pb80_291014_longrun_28001	29/10/20 14	R	50mm diameter bruker standard	0-70°, 0.002°, 28001, 47.75s
paracetamol_291014_longrun_28001	29/10/20 14	R	50mm diameter bruker standard	0-70°, 0.002°, 28001, 47.75s

P80Pb20_291014_longrun_2800 1	29/10/20 14	R	50mm diameter bruker standard	0-70°, 0.002°, 28001, 47.75s
S50Pb50_291014_longrun_2800 1	29/10/20 14	R	50mm diameter bruker standard	0-70°, 0.002°, 28001, 47.75s
Sucrose_291014_longrun_28001	29/10/20 14	R	50mm diameter bruker standard	0-70°, 0.002°, 28001, 47.75s
Caffeine_longrun_32401	09/10/20 14	R	50mm diameter bruker standard	10-80°, 0.002°, 32401, 47.75s
Paracetamol_longrun_32401	09/10/20 14	R	50mm diameter bruker standard	10-80°, 0.002°, 32401, 47.75s
Sucrose_longrun_32401	09/10/20 14	R	50mm diameter bruker standard	10-80°, 0.002°, 32401, 47.75s
S40P60_longrun_32401	09/10/20 14	R	50mm diameter bruker standard	10-80°, 0.002°,

				32401, 47.75s
S80P20_longrun_32401	09/10/20 14	R	50mm diameter bruker standard	10-80°, 0.002°, 32401, 47.75s
Caffeine_shortrun_081014	08/10/20 14	R	50mm diameter bruker standard	10-60°, 0.020°, 2457, 47.75s
Paracetamol_shortrun_081014	08/10/20 14	R	50mm diameter bruker standard	10-60°, 0.020°, 2457, 47.75s
Sucrose_shortrun_081014	08/10/20 14	R	50mm diameter bruker standard	10-60°, 0.020°, 2457, 47.75s
S40P60_shortrun_081014	08/10/20 14	R	50mm diameter bruker standard	10-60°, 0.020°, 2457, 47.75s
S80P20_shortrun_081014	08/10/20 14	R	50mm diameter bruker standard	10-60°, 0.020°, 2457, 47.75s

L50P50_longrun_32401	08/10/20 14	R	50mm diameter bruker standard	10-80°, 0.002°, 32401, 47.75s
S80P20_longrun_32401	08/10/20 14	R	50mm diameter bruker standard	10-80°, 0.002°, 32401, 47.75s
Pb(NO ₂) ₃ _longrun_32401	08/10/20 14	R	50mm diameter bruker standard	10-80°, 0.002°, 32401, 47.75s
Lead nitrate_shortrun	08/10/20 14	R	50mm diameter bruker standard	10-60°, 0.020°, 2457, 47.75s
Caffeine_shortrun	08/10/20 14	R	50mm diameter bruker standard	10-60°, 0.020°, 2457, 47.75s
L50P50_shortrun	08/10/20 14	R	50mm diameter bruker standard	10-60°, 0.020°, 2457, 47.75s
Paracetamol_shortrun	08/10/20 14	R	50mm diameter bruker standard	10-60°, 0.020°, 2457, 47.75s

				2457, 47.75s
S40P60_shortrun	08/10/20 14	R	50mm diameter bruker standard	10-60°, 0.020°, 2457, 47.75s
S80P20_shortrun	08/10/20 14	R	50mm diameter bruker standard	10-60°, 0.020°, 2457, 47.75s
Sucrose_shortrun	08/10/20 14	R	50mm diameter bruker standard	10-60°, 0.020°, 2457, 47.75s
Caffeine_100_longrun_071014	07/10/20 14	R	50mm diameter bruker standard	0-80°, 0.002°, 39301, 9.55s
Paracetamol_100_longrun_0710 14	07/10/20 14	R	50mm diameter bruker standard	0-80°, 0.002°, 39301, 9.55s
Sucrose_100_longrun_071014	07/10/20 14	R	50mm diameter bruker standard	0-80°, 0.002°, 39301, 9.55s

C&P_50&50_070813	07/08/20 13	R	Background Holder	10-60°, 0.020°, 2457, 45.84s
S&C_50&50_070813	07/08/20 13	R	Background Holder	10-60°, 0.020°, 2457, 45.84s
S&P_50&50_070813	07/08/20 13	R	Background Holder	10-60°, 0.020°, 2457, 45.84s
paracetamol_100%_070813	07/08/20 13	R	Background Holder	10-60°, 0.020°, 2457, 45.84s
Caffeine_100%_070813	07/08/20 13	R	Background Holder	10-60°, 0.020°, 2457, 45.84s
Sucrose_100%_070813	07/08/20 13	R	Background Holder	10-60°, 0.020°, 2457, 45.84s
Morphine290413	29/04/20 13	R	Background Holder	10-60°, 0.020°,

				2457, 45.84s
Morphine1_290413	29/04/20 13	R	Background Holder	10-60°, 0.020°, 2457, 45.84s
Noscapine1_290413	29/04/20 13	R	Background Holder	10-60°, 0.020°, 2457, 45.84s
Paracetamol1_290413	29/04/20 13	R	Background Holder	10-60°, 0.020°, 2457, 45.84s
Sucrose1_290413	29/04/20 13	R	Background Holder	10-60°, 0.020°, 2457, 45.84s